Chapter 7

Modeling Biogas Plants

In this chapter the simulation model of the biogas plant used inside the model predictive control (Chapter 2) and used for performance evaluation of the control using simulations (chapters 8 and 9) is presented. The most important part of a biogas plant model is the model of the anaerobic digestion process. In this thesis the Anaerobic Digestion Model No. 1 (ADM1) is used for that purpose (Section 7.1). The ADM1 is the nowadays most often used and most complex simulation model of the AD process. The complexity of the ADM1 allows a very detailed characterization of the substrate feed, which is very important for a realistic model representation of the real world (Section 7.2). A biogas plant is a system where energy is produced (in case the produced biogas is burned in combined heat and power plants (CHPs): electrical and thermal energy) and where energy is consumed. Typical energy sinks are pumps, stirrers and the heat losses through the digester insulation. The produced energy is usually sold, such that economic issues must be included in the model as well. As all such aspects determine how well a biogas plant is operated those criteria are performance indicators, whose models are described in Section 7.3.
In Section 7.4 the implementation of a model of a full-scale biogas plant, developed in MATLAB®, is shown. The calibration and validation of that model on real data is discussed in Section 7.5.
Next to the ADM1 there are many other models of the anaerobic digestion process, all started with the model of Andrews (1968). As there are a lot of excellent reviews on such models in this thesis the author does without a review, but refers to the reviews in Appels et al. (2008), Dewil et al. (2011), Donoso-Bravo et al. (2011), Gavala et al. (2003), Gerber and Span (2008), Gerber (2009), Lauwers et al. (2013), Lübken et al. (2010), Saravanan and Sreekrishnan (2006), Tomei et al. (2009) and Wolf (2013).

General Remark on Notation To avoid tedious formalism all definitions and equations in this chapter assume that the biogas plant only contains one anaerobic digester which is fed with one single substrate and the biogas is burned in one combined

heat and power plant. Nevertheless all definitions can easily be generalized for a biogas plant with more than one digester, substrate and CHP. In this generalized manner the algorithms, modeling each biogas plant, are implemented (see Part B of the appendix). Here, this simplification is only done to clean up the notation.

7.1 The Anaerobic Digestion Model No. 1 (ADM1)

The Anaerobic Digestion Model No. 1 was published by a Task Group of the International Water Association in 2002, (Batstone et al., 2002a,b). It can be seen as a merger of all previously published AD models and is since then established as the standard model for the AD process.

The ADM1 models the anaerobic digestion process in 19 biochemical processes, six acid/base equilibria, three liquid/gas transfer processes and one for the pressure in the gas phase. The 19 biochemical processes include the main chemical reactions of the four steps of anaerobic digestion described in Section 5.1. They are preceded by a disintegration step, which models the physical breakup of the substrates into their biomolecules. For a CSTR (Section 5.4.1) the ADM1 can be modeled as an ordinary differential equation (ODE) system as given in equation (7.1) with the definitions of the ADM1 state vector ${}^{o}\boldsymbol{x}_{\mathrm{AD}} : \mathbb{R}^{+} \to \mathbb{R}^{37}$ and the ADM1 input vector ${}^{o}\boldsymbol{u}_{\mathrm{AD}} : \mathbb{R}^{+} \to \mathbb{R}^{34}$ in eq. (7.2).

$$ {}^{o}\boldsymbol{x}_{\mathrm{AD}}{}'(\tau) = \boldsymbol{D}_u(\tau) \cdot {}^{o}\boldsymbol{u}_{\mathrm{AD}}(\tau) - \boldsymbol{D}_x(\tau) \cdot {}^{o}\boldsymbol{x}_{\mathrm{AD}}(\tau) + \boldsymbol{V}\left({}^{o}\boldsymbol{x}_{\mathrm{AD}}\right)^{T} \cdot \boldsymbol{\rho}\left({}^{o}\boldsymbol{x}_{\mathrm{AD}}\right) \tag{7.1} $$

The 37 components of the ADM1 state vector ${}^{o}\boldsymbol{x}_{\mathrm{AD}}$ are listed in Table 7.1. The first 33 components of the input ${}^{o}\boldsymbol{u}_{\mathrm{AD}}$ are in the same order as in the state vector ${}^{o}\boldsymbol{x}_{\mathrm{AD}}$, such that in eq. (7.2) the missing input components are abbreviated with dots. The input vector ${}^{o}\boldsymbol{u}_{\mathrm{AD}}$ is modeled in Section 7.2. Please note that, because in the considered case the biogas plant only contains one digester which is fed with one substrate, the state vector ${}^{o}\boldsymbol{x}$ and the input vector $\boldsymbol{u}$, both defined in Chapter 2, are identical to ${}^{o}\boldsymbol{x}_{\mathrm{AD}}$ and ${}^{o}\boldsymbol{u}_{\mathrm{AD}}$, respectively.

$$ \begin{aligned} {}^{o}\boldsymbol{x}_{\mathrm{AD}} &:= \left({}^{o}x_{\mathrm{AD},1}, {}^{o}x_{\mathrm{AD},2}, \ldots, {}^{o}x_{\mathrm{AD},i}, \ldots, {}^{o}x_{\mathrm{AD},37}\right)^{T} \\ {}^{o}\boldsymbol{u}_{\mathrm{AD}} &:= \left(S_{\mathrm{su,IN}}, S_{\mathrm{aa,IN}}, S_{\mathrm{fa,IN}}, S_{\mathrm{va,IN}}, \ldots, S^{-}_{\mathrm{ac,IN}}, S^{-}_{\mathrm{hco3,IN}}, S_{\mathrm{nh3,IN}}, Q_{\mathrm{IN}}\right)^{T} \end{aligned} \tag{7.2} $$

In eq. (7.1) the linear matrix function $\boldsymbol{V} : \mathbb{R}^{37} \to \mathbb{R}^{29\times 37}$ is the stoichiometric matrix and the nonlinear vector function $\boldsymbol{\rho} : \mathbb{R}^{37} \to \mathbb{R}^{29}$ is the vector of the process rates. The input $\boldsymbol{D}_u : \mathbb{R}^{+} \to \mathbb{R}^{37\times 34}$ and state transition matrix $\boldsymbol{D}_x : \mathbb{R}^{+} \to \mathbb{R}^{37\times 37}$ are diagonal matrices with the dilution rate D on their main diagonal. The vector of process rates $\boldsymbol{\rho} := (\rho_1, \ldots, \rho_j, \ldots, \rho_{29})^{T}$ is affected by the available substrate and biomass but is also affected negatively by inhibiting process values such as ammonia, pH and hydrogen. $\boldsymbol{V}, \boldsymbol{\rho}, \boldsymbol{D}_u$ and $\boldsymbol{D}_x$ are defined in the appendix, see Part C.

Using the liquid/gas transfers, biogas production is calculated. The ADM1, in its standard implementation, models biogas as a mixture of the three gases hydrogen (H_2), methane (CH_4) and carbon dioxide (CO_2). Their volumetric flow rates are defined as $Q_{\mathrm{h_2}}, Q_{\mathrm{ch_4}}, Q_{\mathrm{co_2}}$, respectively, and are measured in $\frac{\mathrm{m}^3}{\mathrm{d}}$. The volumetric flow rate of total produced biogas Q_{gas} is defined as the sum of the biogas components, as given in equation (7.3).

$$Q_{\mathrm{gas}} := \sum_{i \in \{\mathrm{h_2}, \mathrm{ch_4}, \mathrm{co_2}\}} Q_i = Q_{\mathrm{h_2}} + Q_{\mathrm{ch_4}} + Q_{\mathrm{co_2}} \qquad [Q_{\mathrm{gas}}] = \frac{\mathrm{m}^3}{\mathrm{d}} \tag{7.3}$$

The relative content r_i of each biogas component $i \in \{\mathrm{h_2}, \mathrm{ch_4}, \mathrm{co_2}\}$ is defined in equation (7.4).

$$r_i := \frac{Q_i}{Q_{\mathrm{gas}}}, \qquad i \in \{\mathrm{h_2}, \mathrm{ch_4}, \mathrm{co_2}\} \qquad [r_i] = 100\ \% \tag{7.4}$$

7.1.1 Extensions of the Anaerobic Digestion Model No. 1

Over the last decade quite a lot of extensions to the ADM1 have been proposed and successfully implemented. Figure 7.1 visualizes the percentage distribution of five different categories of extensions. In total 73 extensions have been found in the literature.

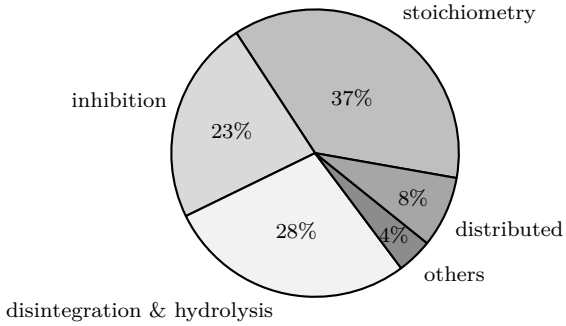

Figure 7.1: Percentage distribution of ADM1 extensions (73 publications).

The **disintegration & hydrolysis** steps are extended to account for different rates of degradability of different substrates and substrate components. The effects of particle size, TS content, thermal and ultrasound pretreatment, start-up behavior and others on the degradation behaviour of substrates were studied.

Process inhibition due to some substances inside the digester is modeled in the ADM1 by continuous **inhibition** functions $I : \mathbb{R}^{37} \to [0, 1]$. They are multiplied with the reaction rate ρ_j of the affected reaction $j \in \{1, \ldots, 19\}$ and return 1, when no inhibition is active. A few more inhibition functions next to the ones already implemented

in the ADM1 were proposed over the last years. Examples are inhibition by total volatile fatty acids, sodium, long chain fatty acids (LCFAs), phenolic compounds and pharmaceuticals.

Extensions affecting the **stoichiometry** of the ADM1 are those that include more processes or make the stoichiometry variable. Examples are precipitation reactions, sulphate and nitrate reduction, inclusion of phenolic compounds, ethanol and lactic acid, variable stoichiometry, microbial storage, acetate oxidation and multi-species models.

On the one hand **distributed** models can be used to model different layers in the reactor (1d-models) and on the other hand they can be used to analyze the interaction between different types of biomass species in sludge granules (2d- and 3d-models).

7.1.2 Applications of the Anaerobic Digestion Model No. 1

The ADM1 was applied to many different substrate feeds in liquid as well as in solid form. In Figure 7.2a the percentage distribution of four different types of substrates can be seen. To the class of liquid wastes belong substrates with a low total solids content. Examples are sewage sludge from wastewater treatment plants and olive pulp. To the wastewater type belong winery, black, paper mill as well as synthetic wastewater. Agricultural substrates are those mainly fed on agricultural biogas plants. Examples are grass silage, different crops and all sorts of manure. Finally, solid wastes are the organic fraction of municipal solid wastes (OFMSW) as well as vegetable/kitchen waste.

The digestion temperature most of the time is in the mesophilic temperature region as is visualized in Figure 7.2b. Most reactors are continuously stirred (CSTR) as is

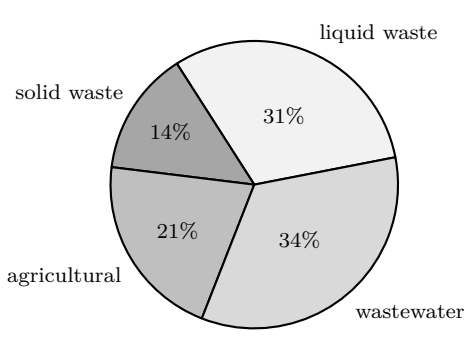

(a) Types of substrate feeds (142 publications)

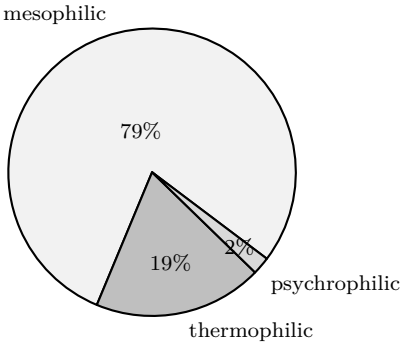

(b) Digestion temperature (119 publications)

Figure 7.2: Applications of the ADM1: Part I

depicted in Figure 7.3a. To them also all lab experiments performed in e.g. bottles or

vessels belong. The ADM1 most of the time is calibrated to lab-scale experiments, but pilot- as well as full-scale applications have a fair share of all applications as well, see Figure 7.3b.

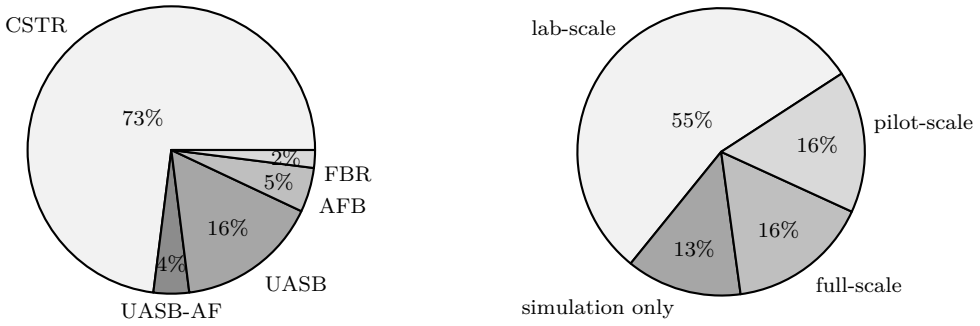

(a) Types of reactors (111 publications) **(b)** Scale of reactors (142 publications)

Figure 7.3: Applications of the ADM1: Part II

In all these applications different implementations of the Anaerobic Digestion Model No. 1 were used and also the substrate characteristics were modeled differently. But, so far, it seems that all these applications could be modeled with some ADM1 implementation with sufficient accuracy. At the moment a best practice guide on how to model a biogas plant properly using the ADM1 with different types of substrates (liquid, solid) is not there yet.

The references to all publications used to create the charts in this and the previous subsection can be found here[1].

7.1.3 Implementation of the ADM1 in this Work

In this thesis basically the ADM1 implementation of Simba 6.4, Tschepetzki and Ogurek (2010), is used. This is an implementation of the ADM1 as system of ODEs with the extension proposed in Wett et al. (2006). The following further extensions were added to the model.

To account for the loss of mass, which is released with the produced biogas, the volumetric flow rate of the substrate feed is reduced by the mass loss of the expected biogas production as suggested in Koch (2010). To not change the substrate feed parameters the input concentrations in ${}^{o}\boldsymbol{u}_{\mathrm{AD}}$ are multiplied with the inverse of the mass reduction factor. Using this change it is possible to model the fill-level of the digester. Koch (2010) furthermore suggests a TS dependent hydrolysis (affecting the

[1] `http://www.mendeley.com/groups/3709301/anaerobic-digestion-model-no-1/`

process rates ρ_j with $j = 2, 3, 4$) using equation (7.5), which is implemented as well. In eq. (7.5) the bijection $j_S : \{2, 3, 4\} \to \{\mathrm{ch}, \mathrm{pr}, \mathrm{li}\}$ is used.

$$\underbrace{\rho_j = k_{\mathrm{hyd},j_S(j)} \cdot X_{j_S(j)}}_{\text{original ADM1 eq.}} \cdot \frac{1}{1 + \left(\frac{\mathrm{TS}}{K_{\mathrm{hyd}}}\right)^{n_{\mathrm{hyd}}}} \tag{7.5}$$

There the inhibition constant of hydrolysis K_{hyd}, $[K_{\mathrm{hyd}}] = \%_{\mathrm{FM}}$, and the inhibition index of hydrolysis n_{hyd}, $[n_{\mathrm{hyd}}] = 100\ \%$, are used.

Table 7.1: State vector components ${}^{o}x_{\mathrm{AD},i}$ of the ADM1 (Tschepetzki and Ogurek, 2010)

i	${}^{o}x_{\mathrm{AD},i}$	Description	Unit
1	S_{su}	monosaccharides	$\mathrm{kg_{COD}} \cdot \mathrm{m}^{-3}$
2	S_{aa}	amino acids	$\mathrm{kg_{COD}} \cdot \mathrm{m}^{-3}$
3	S_{fa}	total long chain fatty acids (LCFA)	$\mathrm{kg_{COD}} \cdot \mathrm{m}^{-3}$
4	S_{va}	valeric acid S_{hva} + valerate; $S_{\mathrm{hva}} := S_{\mathrm{va}} - S_{\mathrm{va}}^{-}$	$\mathrm{kg_{COD}} \cdot \mathrm{m}^{-3}$
5	S_{bu}	butyric acid S_{hbu} + butyrate; $S_{\mathrm{hbu}} := S_{\mathrm{bu}} - S_{\mathrm{bu}}^{-}$	$\mathrm{kg_{COD}} \cdot \mathrm{m}^{-3}$
6	S_{pro}	propionic acid S_{hpro} + propionate; $S_{\mathrm{hpro}} := S_{\mathrm{pro}} - S_{\mathrm{pro}}^{-}$	$\mathrm{kg_{COD}} \cdot \mathrm{m}^{-3}$
7	S_{ac}	acetic acid S_{hac} + acetate; $S_{\mathrm{hac}} := S_{\mathrm{ac}} - S_{\mathrm{ac}}^{-}$	$\mathrm{kg_{COD}} \cdot \mathrm{m}^{-3}$
8	S_{h2}	hydrogen	$\mathrm{kg_{COD}} \cdot \mathrm{m}^{-3}$
9	S_{ch4}	methane	$\mathrm{kg_{COD}} \cdot \mathrm{m}^{-3}$
10	S_{co2}	carbon dioxide	$\mathrm{kmol} \cdot \mathrm{m}^{-3}$
11	S_{nh4}^{+}	ammonium	$\mathrm{kmol} \cdot \mathrm{m}^{-3}$
12	S_{I}	soluble inerts	$\mathrm{kg_{COD}} \cdot \mathrm{m}^{-3}$
13	X_{c}	composite	$\mathrm{kg_{COD}} \cdot \mathrm{m}^{-3}$
14	X_{ch}	carbohydrates	$\mathrm{kg_{COD}} \cdot \mathrm{m}^{-3}$
15	X_{pr}	proteins	$\mathrm{kg_{COD}} \cdot \mathrm{m}^{-3}$
16	X_{li}	lipids	$\mathrm{kg_{COD}} \cdot \mathrm{m}^{-3}$
17	X_{su}	biomass of sugar degraders	$\mathrm{kg_{COD}} \cdot \mathrm{m}^{-3}$
18	X_{aa}	biomass of amino acids degraders	$\mathrm{kg_{COD}} \cdot \mathrm{m}^{-3}$
19	X_{fa}	biomass of LCFA degraders	$\mathrm{kg_{COD}} \cdot \mathrm{m}^{-3}$
20	X_{c4}	biomass of valerate + butyrate degraders	$\mathrm{kg_{COD}} \cdot \mathrm{m}^{-3}$
21	X_{pro}	biomass of propionate degraders	$\mathrm{kg_{COD}} \cdot \mathrm{m}^{-3}$
22	X_{ac}	biomass of acetate degraders	$\mathrm{kg_{COD}} \cdot \mathrm{m}^{-3}$
23	X_{h2}	biomass of hydrogen degraders	$\mathrm{kg_{COD}} \cdot \mathrm{m}^{-3}$
24	X_{I}	particulate inerts	$\mathrm{kg_{COD}} \cdot \mathrm{m}^{-3}$
25	X_{p}	particulate products arising from biomass decay	$\mathrm{kg_{COD}} \cdot \mathrm{m}^{-3}$
26	S_{cat}^{+}	cations	$\mathrm{kmol} \cdot \mathrm{m}^{-3}$
27	S_{an}^{-}	anions	$\mathrm{kmol} \cdot \mathrm{m}^{-3}$
28	S_{va}^{-}	valerate	$\mathrm{kg_{COD}} \cdot \mathrm{m}^{-3}$
29	S_{bu}^{-}	butyrate	$\mathrm{kg_{COD}} \cdot \mathrm{m}^{-3}$
30	S_{pro}^{-}	propionate	$\mathrm{kg_{COD}} \cdot \mathrm{m}^{-3}$
31	S_{ac}^{-}	acetate	$\mathrm{kg_{COD}} \cdot \mathrm{m}^{-3}$
32	S_{hco3}^{-}	bicarbonate	$\mathrm{kmol} \cdot \mathrm{m}^{-3}$
33	S_{nh3}	ammonia	$\mathrm{kmol} \cdot \mathrm{m}^{-3}$
34	$\mathrm{pi}_{\mathrm{Sh2}}$	partial pressure of S_{h2}	bar
35	$\mathrm{pi}_{\mathrm{Sch4}}$	partial pressure of S_{ch4}	bar
36	$\mathrm{pi}_{\mathrm{Sco2}}$	partial pressure of S_{co2}	bar
37	$\mathrm{p}_{\mathrm{total}}$	sum of all partial pressures	bar

7.2 The Substrate Feed

The substrate feed of the biogas plant is modeled as the input vector ${}^{o}\boldsymbol{u}_{\mathrm{AD}}$ defined in equation (7.2). If the biogas plant is fed with more than one substrate, ${}^{o}\boldsymbol{u}_{\mathrm{AD}}$ contains a weighted sum of the substrates concentrations, weighted by the fed amount of each substrate. Most components of the input vector ${}^{o}\boldsymbol{u}_{\mathrm{AD}}$ are measured as COD (Section 5.3.3) concentrations, which is a very common measurement in wastewater treatment. For agricultural substrates measuring the chemical oxygen demand is not that usual. In agriculture it is more common to analyze the cell content of the substrate by the extended Weender analysis (Van Soest et al., 1991), see Table 7.2. Using the approach in Koch et al. (2010) the particulate COD of the substrate can be calculated out of the cell components, see Subsection 7.2.1. In Table 7.3 all measurement values used for the full substrate characterization are listed.

Table 7.2: In the extended Weender analysis the substrate is determined by the depicted components (cf. Schuldt and Dinse (2010), Koch et al. (2010)).

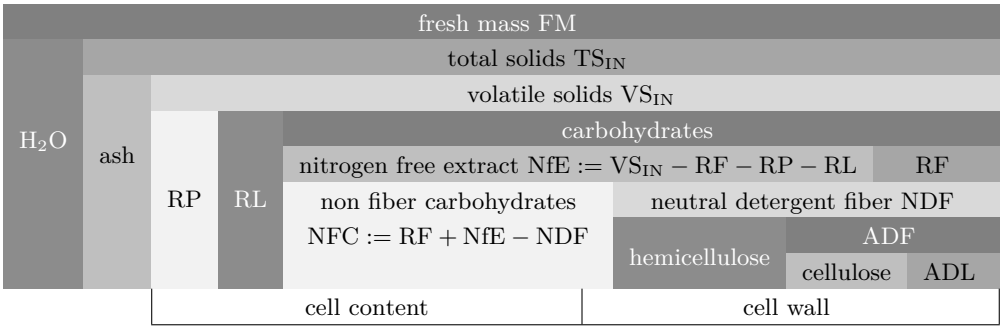

7.2.1 COD containing Input Variables

The total chemical oxygen demand in the substrate $\mathrm{COD}_{\mathrm{total}}$ exists as soluble COD and particulate chemical oxygen demand $\mathrm{COD}_{\mathrm{X}}$, all measured in $\frac{\mathrm{kg}_{\mathrm{COD}}}{\mathrm{m}^3}$. The particulate COD of the substrate $\mathrm{COD}_{\mathrm{X}}$ is approximated using equation (7.6) as suggested in Koch (2010). ThOD_i, $i \in \{\mathrm{pr}, \mathrm{li}, \mathrm{l}, \mathrm{ch}\}$, denote the theoretical oxygen demand of protein, lipids, lignin and carbohydrates, respectively (Section 5.3.9).

$$\mathrm{COD}_{\mathrm{X}} \approx \rho_{\mathrm{IN}} \cdot \mathrm{TS}_{\mathrm{IN}} \cdot \underbrace{\left(\begin{array}{c} \mathrm{RP} \cdot \mathrm{ThOD}_{\mathrm{pr}} + \mathrm{RL} \cdot \mathrm{ThOD}_{\mathrm{li}} + \mathrm{ADL} \cdot \mathrm{ThOD}_{\mathrm{l}} + \\ + (\mathrm{RF} + \mathrm{NfE} - \mathrm{ADL}) \cdot \mathrm{ThOD}_{\mathrm{ch}} \end{array}\right)}_{=:\mathrm{VS}_{\mathrm{IN}} \cdot \overline{\mathrm{ThOD}} \quad \text{used later in eq. (7.57)}} \tag{7.6}$$

In equation (7.6) the density of the substrate ρ_{IN} is needed, which is modeled in equation (7.7). Values for the needed single densities $\rho_{\mathrm{pr}}, \rho_{\mathrm{li}}, \ldots$ to calculate the density

Table 7.3: Measured parameters for substrate feed characterization

Symbol	Description (... of/in substrate)	Unit	Method
TS_{IN}	total solids (Section 5.3.10)	$\%_{FM}$	DIN EN 12880, DIN (2001a)
VS_{IN}	volatile solids (Section 5.3.11)	$\%_{TS}$	DIN EN 12879, DIN (2001b)
RP	raw protein	$\%_{TS}$	VDLUFA (1997) III 4.1.1
RL	raw lipids	$\%_{TS}$	VDLUFA (1997) III 5.1.1
NDF	neutral detergent fiber	$\%_{TS}$	VDLUFA (1997) III 6.5.1
ADF	acid detergent fiber	$\%_{TS}$	VDLUFA (1997) III 6.5.2
ADL	acid detergent lignin	$\%_{TS}$	VDLUFA (1997) III 6.5.3
$pH_{IN} \in \mathbb{R}^+$	pH value	–	DIN EN 12176, DIN (1998)
$S^+_{nh4,IN}$	ammonium value	$\frac{mol}{l}$	DIN 38406-5, DIN (1983)
TA_{IN}	total alkalinity	$\frac{mmol}{l}$	DIN 38409-7, DIN (2005)
T_{IN}	temperature	^oC	DIN 38404-4, DIN (1976)
$S_{va,IN}$	valeric acid	$\frac{g}{l}$	gas chromatography (GC)
$S_{bu,IN}$	butyric acid	$\frac{g}{l}$	GC, BMU (2012b)
$S_{pro,IN}$	propionic acid	$\frac{g}{l}$	GC, BMU (2012b)
$S_{ac,IN}$	acetic acid	$\frac{g}{l}$	GC, BMU (2012b)
$D_{VS} \in [0,1]$	degradation level	100 %	Koch et al. (2009)
k_{dis}	disintegration rate	$\frac{1}{d}$	difficult to determine,
$k_{hyd,ch}$	hydrolysis rate carbohydrates	$\frac{1}{d}$	see discussion in
$k_{hyd,pr}$	hydrolysis rate protein	$\frac{1}{d}$	Astals et al. (2013) (k_{dis})
$k_{hyd,li}$	hydrolysis rate lipids	$\frac{1}{d}$	and Batstone et al. (2009)
$COD_{filtrate}$	total COD of filtrate	$\frac{kg_{COD}}{m^3}$	DIN ISO 15705, DIN (2003)
$S_{I,IN}$	soluble inerts	$\frac{kg_{COD}}{m^3}$	Ince et al. (1998)
p_{IN}	substrate costs	$\frac{€}{t}$	-

of the substrate ρ_{IN}, $[\rho_{IN}] = \frac{kg_{FM}}{m^3}$, can be found in Gerber (2009).

$$\rho_{IN} = TS_{IN} \cdot \begin{pmatrix} RP \cdot \rho_{pr} + RL \cdot \rho_{li} + (RF + NfE) \cdot \rho_{ch} + \\ + (1 - VS_{IN}) \cdot \rho_{ash} \end{pmatrix} + (1 - TS_{IN}) \cdot \rho_{H_2O} \quad (7.7)$$

The raw fiber content RF of the substrate is not needed in this approach, because in all equations (e.g. eqs. (7.6) and (7.11)) only the sum RF + NfE is needed, which per definition (Table 7.2) is equal to $VS_{IN} - RP - RL$ and thus can be calculated.
As Figure 7.4 visualizes, the total chemical oxygen demand COD_{total} of the substrate is split into disintegrated and non-disintegrated COD. The disintegrated chemical oxygen demand is approximated by the COD of the filtrate $COD_{filtrate}$, which contains the soluble COD as well. Soluble COD in the substrate is solely assumed to be existent in the form of the short chain fatty acids (SCFAs) $S_{va,IN}, S_{bu,IN}, S_{pro,IN}$ and $S_{ac,IN}$ as well as soluble inerts $S_{I,IN}$, which all have to be measured, see Table 7.3. The other soluble

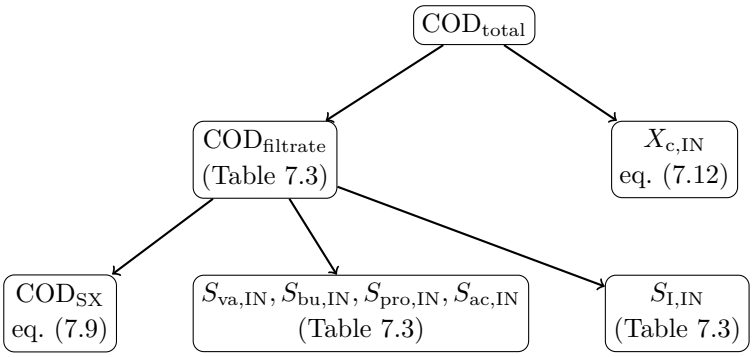

Figure 7.4: Fragmentation of total COD of substrate $\mathrm{COD_{total}}$.

COD components are assumed to be zero, see equation (7.8).

$$S_{\mathrm{su,IN}} = S_{\mathrm{aa,IN}} = S_{\mathrm{fa,IN}} = S_{\mathrm{h2,IN}} = S_{\mathrm{ch4,IN}} = 0 \ \frac{\mathrm{kg_{COD}}}{\mathrm{m^3}} \tag{7.8}$$

The disintegrated particulate COD, which is the disintegrated COD excluding the soluble COD, is symbolized by $\mathrm{COD_{SX}}$, $[\mathrm{COD_{SX}}] = \frac{\mathrm{kg_{COD}}}{\mathrm{m^3}}$, and given as

$$\mathrm{COD_{SX}} \approx \mathrm{COD_{filtrate}} - S_{\mathrm{va,IN}} - S_{\mathrm{bu,IN}} - S_{\mathrm{pro,IN}} - S_{\mathrm{ac,IN}} - S_{\mathrm{I,IN}}. \tag{7.9}$$

$\mathrm{COD_{SX}}$ is used in equation (7.10) to calculate the COD fractions of carbohydrates, proteins and lipids.

$$\begin{aligned} X_{\mathrm{ch,IN}} &= \frac{\mathrm{COD_{SX}}}{f_{\mathrm{ch,Xc}} + f_{\mathrm{pr,Xc}} + f_{\mathrm{li,Xc}}} \cdot (f_{\mathrm{ch,Xc}} + f_{\mathrm{li,Xc}} \cdot (1 - f_{\mathrm{fa,li}})) \\ X_{\mathrm{pr,IN}} &= \frac{\mathrm{COD_{SX}}}{f_{\mathrm{ch,Xc}} + f_{\mathrm{pr,Xc}} + f_{\mathrm{li,Xc}}} \cdot f_{\mathrm{pr,Xc}} \\ X_{\mathrm{li,IN}} &= \frac{\mathrm{COD_{SX}}}{f_{\mathrm{ch,Xc}} + f_{\mathrm{pr,Xc}} + f_{\mathrm{li,Xc}}} \cdot f_{\mathrm{li,Xc}} \cdot f_{\mathrm{fa,li}} \end{aligned} \tag{7.10}$$

In equation (7.10) the fractions given in equation (7.11)

$$\begin{aligned} f_{\mathrm{pr,Xc}} &:= \frac{\mathrm{RP}}{\mathrm{VS_{IN}}} \in [0,1] \\ f_{\mathrm{li,Xc}} &:= \frac{\mathrm{RL}}{\mathrm{VS_{IN}}} \in [0,1] \\ f_{\mathrm{ch,Xc}} &:= \frac{(\mathrm{RF} + \mathrm{NfE} - \mathrm{NDF}) + (\mathrm{NDF} - \mathrm{ADL}) \cdot d}{\mathrm{VS_{IN}}} \in [0,1] \\ f_{\mathrm{xi,Xc}} &:= \frac{\mathrm{ADL} + (\mathrm{NDF} - \mathrm{ADL}) \cdot (1-d)}{\mathrm{VS_{IN}}} \in [0,1]\,, \end{aligned} \tag{7.11}$$

$f_{\mathrm{fa,li}} = 0.95$, $d = \frac{\mathrm{NDF} - \mathrm{VS_{IN}} \cdot (1 - D_{\mathrm{VS}})}{\mathrm{NDF} - \mathrm{ADL}} \in [0,1]$ and $f_{\mathrm{pr,Xc}} + f_{\mathrm{li,Xc}} + f_{\mathrm{ch,Xc}} + f_{\mathrm{xi,Xc}} = 1$ are used, Koch et al. (2010). The non-disintegrated part of the particulate chemical oxygen demand $\mathrm{COD_X}$ is modeled as the ADM1 input component $X_{\mathrm{c,IN}}$ and is given

in equation (7.12).

$$X_{\mathrm{c,IN}} = \mathrm{COD_X} - \mathrm{COD_{SX}} \tag{7.12}$$

The following particulate inputs are set to zero:

$$X_{\mathrm{I,IN}} = X_{\mathrm{p,IN}} = 0 \ \frac{\mathrm{kg_{COD}}}{\mathrm{m^3}}.$$

If the substrate is some sort of manure the biomass in the substrate is calculated as suggested in Lübken et al. (2007b) and subtracted from $X_{\mathrm{c,IN}}$. The biomasses $X_{\mathrm{su,IN}}, X_{\mathrm{aa,IN}}, X_{\mathrm{fa,IN}}, X_{\mathrm{c4,IN}}, X_{\mathrm{pro,IN}}, X_{\mathrm{ac,IN}}$ and $X_{\mathrm{h2,IN}}$ are set to equal ratios of the calculated values in Lübken et al. (2007b). If the substrate is not manure, then all mentioned biomass fractions are set to 0 $\frac{\mathrm{kg_{COD}}}{\mathrm{m^3}}$.

The ionized SCFAs are set in eq. (7.13) by the acid/base equilibria using the measured acid concentrations and the dissociation constants $pK_{S_{\mathrm{va}}}, pK_{S_{\mathrm{bu}}}, pK_{S_{\mathrm{pro}}}$ and $pK_{S_{\mathrm{ac}}} \in \mathbb{R}^+$.

$$\begin{aligned}
S^-_{\mathrm{va,IN}} &= \frac{S_{\mathrm{va,IN}}}{1 + 10^{pK_{S_{\mathrm{va}}} - \mathrm{pH_{IN}}}} & \left[S^-_{\mathrm{va,IN}}\right] &= \frac{\mathrm{kg_{COD}}}{\mathrm{m^3}} \\
S^-_{\mathrm{bu,IN}} &= \frac{S_{\mathrm{bu,IN}}}{1 + 10^{pK_{S_{\mathrm{bu}}} - \mathrm{pH_{IN}}}} & \left[S^-_{\mathrm{bu,IN}}\right] &= \frac{\mathrm{kg_{COD}}}{\mathrm{m^3}} \\
S^-_{\mathrm{pro,IN}} &= \frac{S_{\mathrm{pro,IN}}}{1 + 10^{pK_{S_{\mathrm{pro}}} - \mathrm{pH_{IN}}}} & \left[S^-_{\mathrm{pro,IN}}\right] &= \frac{\mathrm{kg_{COD}}}{\mathrm{m^3}} \\
S^-_{\mathrm{ac,IN}} &= \frac{S_{\mathrm{ac,IN}}}{1 + 10^{pK_{S_{\mathrm{ac}}} - \mathrm{pH_{IN}}}} & \left[S^-_{\mathrm{ac,IN}}\right] &= \frac{\mathrm{kg_{COD}}}{\mathrm{m^3}}
\end{aligned} \tag{7.13}$$

7.2.2 Other Input Variables

The components of the input vector ${}^o\boldsymbol{u}_{\mathrm{AD}}$ that are not measured in COD concentrations are modeled as follows. The input concentration of bicarbonate $S^-_{\mathrm{hco3,IN}}$, $\left[S^-_{\mathrm{hco3,IN}}\right] = \frac{\mathrm{kmol}}{\mathrm{m^3}}$, is calculated out of the measured total alkalinity value $\mathrm{TA_{IN}}$ according to equation (7.14), which comes directly out of the definition of the TA value in equation (7.61).

$$S^-_{\mathrm{hco3,IN}} = \mathrm{TA_{IN}} - S^-_{\mathrm{an,IN}} - S^-_{\mathrm{ac,IN}} - S^-_{\mathrm{pro,IN}} - S^-_{\mathrm{bu,IN}} - S^-_{\mathrm{va,IN}} + S^+_{\mathrm{cat,IN}} \tag{7.14}$$

The soluble CO_2 concentration $S_{\mathrm{co2,IN}}$ is calculated out of the acid/base equilibrium in equation (7.15), Berg et al. (2007).

$$S_{\mathrm{co2,IN}} = 10^{6.3 - \mathrm{pH_{IN}}} \cdot S^-_{\mathrm{hco3,IN}} \qquad [S_{\mathrm{co2,IN}}] = \frac{\mathrm{kmol}}{\mathrm{m^3}} \tag{7.15}$$

The ammonia concentration $S_{\mathrm{nh3,IN}}$ is calculated out of the measured ammonium value $S^+_{\mathrm{nh4,IN}}$ using the ammonia/ammonium equilibrium, eq. (7.16) (Karlson et al., 2005).

$$S_{\mathrm{nh3,IN}} = 10^{\mathrm{pH_{IN}} - 9.25} \cdot S^+_{\mathrm{nh4,IN}} \qquad [S_{\mathrm{nh3,IN}}] = \frac{\mathrm{kmol}}{\mathrm{m^3}} \tag{7.16}$$

Finally, the input variables $S^+_{\text{cat,IN}}$ and $S^-_{\text{an,IN}}$ are set such that the pH value calculated from the input stream ${}^o\boldsymbol{u}_{\text{AD}}$ (see Section 7.3.3.3) is equal to the measured pH value pH_{IN} of the substrate (Kleerebezem and Van Loosdrecht, 2006).

7.3 Performance Indicators of Biogas Plants

Apart from the anaerobic digestion process, which is modeled by the ADM1, also energy related components such as CHPs and stirrer (Section 7.3.1), financial issues (Section 7.3.2) as well as other physical and chemical models (Section 7.3.3) are included in the biogas plant model. They are described in this section.

7.3.1 Energy

7.3.1.1 Electrical and Thermal Energy Production

The produced electrical P_{el} and thermal power P_{th} of a combined heat and power plant are modeled using the following two equations (7.17) and (7.18), respectively (cf. Gerber (2009)).

$$P_{\text{el}} = \eta_{\text{el}} \cdot h_{v,h} \cdot Q_{\text{gas}} \qquad [P_{\text{el}}] = \frac{\text{kWh}}{\text{d}} \tag{7.17}$$

$$P_{\text{th}} = \eta_{\text{th}} \cdot h_{v,h} \cdot Q_{\text{gas}} \qquad [P_{\text{th}}] = \frac{\text{kWh}}{\text{d}} \tag{7.18}$$

Values for the electrical η_{el} and thermal degree of efficiency η_{th} are found in data sheets of combined heat and power plants; $[\eta_{\text{el}}] = [\eta_{\text{th}}] = 100\ \%$. Both values must be given with respect to the higher heating value $h_{v,h}$, otherwise the lower heating value must be used in eqs. (7.17) and (7.18) instead. The volumetric flow rate of the produced biogas Q_{gas} is returned by the ADM1 (eq. (7.3)).
The higher heating value $h_{v,h}$ of the produced biogas is defined as the weighted sum of the higher heating values $h_{v,h,i}$ of the $i \in \{\text{h}_2, \text{ch}_4, \text{co}_2\}$ biogas components (eq. (7.19)) (DIN, 1997). The weights are given by the gas concentrations r_i (eq. (7.4)) of the i gas components.

$$h_{v,h} := \sum_{i \in \{\text{h}_2, \text{ch}_4, \text{co}_2\}} r_i \cdot h_{v,h,i} \qquad [h_{v,h}] = \frac{\text{kWh}}{\text{m}^3}, \quad [r_i] \stackrel{!}{=} 100\ \% \tag{7.19}$$

7.3.1.2 Electrical Energy Consumption of Agitator

The mechanical power of an agitator P_{mix} needed to mix the content of a digester is calculated in equation (7.20) (Gerber, 2009). The agitator has a diameter d_{mix}, a rotation speed n_{mix}, $[n_{\text{mix}}] = \frac{1}{\text{s}}$, and the density of the sludge inside the digester is approximated by $\rho_{\text{digester}} \approx 1000\ \frac{\text{kg}}{\text{m}^3}$.

$$P_{\text{mix}} = N_{\text{p}} \cdot \rho_{\text{digester}} \cdot {n_{\text{mix}}}^3 \cdot {d_{\text{mix}}}^5 \qquad [P_{\text{mix}}] = \text{W} \tag{7.20}$$

There is a relation between the Newton (or power) number N_p and the Reynolds number Re, which can be determined using the characteristic curve of the agitator. For a stirred vessel the Reynolds number Re is defined in equation (7.21) with the effective viscosity η_eff (Gerber, 2009).

$$Re := \frac{\rho_\mathrm{digester} \cdot n_\mathrm{mix} \cdot {d_\mathrm{mix}}^2}{\eta_\mathrm{eff}} \qquad [Re] = 100\ \% \tag{7.21}$$

For a total solids content TS inside the digester of 3 $\%_\mathrm{FM}$ or higher the effective viscosity η_eff can be calculated using equation (7.22) (Gerber, 2009), $[n_\mathrm{mix}] \stackrel{!}{=} \mathrm{s}^{-1}$.

$$\eta_\mathrm{eff} = \alpha_T \cdot K_\mathrm{c} \cdot \left(\frac{11}{2 \cdot \pi} \cdot n_\mathrm{mix}\right)^{n_\mathrm{flow}-1} \cdot \left(\frac{3 \cdot n_\mathrm{flow} + 1}{4 \cdot n_\mathrm{flow}}\right)^{n_\mathrm{flow}} \qquad [\eta_\mathrm{eff}] = \mathrm{mPa{\cdot}s} \tag{7.22}$$

The consistency coefficient K_c, flow index n_flow and temperature correction α_T are given in equations (7.23) to (7.25) (Gerber, 2009). In these equations the TS content (see eq. (7.57)) and the temperature T inside the digester are used. The units in the three equations must be $[\mathrm{TS}] \stackrel{!}{=} \%_\mathrm{FM}$ and $[T] \stackrel{!}{=} {}^o\mathrm{C}$.

$$K_\mathrm{c} := C_{K_\mathrm{c},1} \cdot \exp\left(C_{K_\mathrm{c},2} \cdot \{\mathrm{TS}\}\right) \qquad [K_\mathrm{c}] = \mathrm{Pa \cdot s} \tag{7.23}$$

$$n_\mathrm{flow} := C_{n_\mathrm{flow},1} \cdot \exp\left(-C_{n_\mathrm{flow},2} \cdot \{\mathrm{TS}\}\right) \qquad [n_\mathrm{flow}] = 100\ \% \tag{7.24}$$

$$\alpha_T := C_{T,1} \cdot \exp\left(-C_{T,2} \cdot \{T\}\right) \qquad [\alpha_T] = 100\ \% \tag{7.25}$$

Values for the substrate dependent coefficients $C_{K_\mathrm{c},1}, C_{K_\mathrm{c},2}, C_{n_\mathrm{flow},1}, C_{n_\mathrm{flow},2}, C_{T,1}$ and $C_{T,2}$ can be found in Türk (1994) and Gerber (2009).

If no characteristic curve for the given agitator is available, the Newton number N_p can also be calculated approximately out of the Reynolds number Re. According to Plank (1988) the following relations hold for the submersible agitator

$$N_\mathrm{p} \approx \begin{cases} \frac{50}{Re} & 1 \le Re < 3.1 \\ \frac{4}{[\log_{10}(Re)]^2} & 3.1 \le Re \le 2 \cdot 10^4 \end{cases} \qquad [N_\mathrm{p}] = 100\ \% \tag{7.26}$$

and the central mixer, both for using a baffle only,

$$N_\mathrm{p} \approx \begin{cases} \frac{80}{Re} & 1 \le Re < 40 \\ 2 & 40 \le Re \le 10^5. \end{cases} \qquad [N_\mathrm{p}] = 100\ \% \tag{7.27}$$

With the mechanical power P_mix of the agitator calculated in equation (7.20), the electrical power input of the stirrer P_MIX is then given by

$$P_\mathrm{MIX} := \frac{P_\mathrm{mix}}{\eta_\mathrm{mix}} \cdot \tau_\mathrm{mix} \qquad [P_\mathrm{MIX}] = \frac{\mathrm{kWh}}{\mathrm{d}} \tag{7.28}$$

with the electrical degree of efficiency for the stirrer η_mix, measured in 100 % and the runtime of the stirrer τ_mix, $[\tau_\mathrm{mix}] = \frac{\mathrm{h}}{\mathrm{d}}$.

7.3.1.3 Dissipation Agitator

The power P_{diss}, which is dissipated by the stirrer inside the digester, is assumed to be equal to the mechanical power of the stirrer needed to mix the sludge inside the digester P_{mix} (eq. (7.20)), Gerber (2009).

$$P_{\text{diss}} = P_{\text{mix}} \cdot \tau_{\text{mix}} \qquad [P_{\text{diss}}] = \frac{\text{kWh}}{\text{d}} \tag{7.29}$$

7.3.1.4 Electrical Energy Consumption of Substrate and Sludge Transport

Pumps The electrical power P_{pump} needed to pump a volumetric flow rate Q of liquid substrate or sludge is calculated in equation (7.30) (Gerber, 2009). There, the energy needed to lift the material by the geodetic head of the pump Δh_{geo}, $[\Delta h_{\text{geo}}] = \text{m}$, and to transport it by a distance l_{pipe} is calculated, assuming an electrical degree of efficiency of the pump η_{pump}, $[\eta_{\text{pump}}] = 100\ \%$. The density ρ of substrates is calculated as in equation (7.7) and the density of sludge is approximated with $\rho \approx 1000\ \frac{\text{kg}}{\text{m}^3}$. g is the gravitational acceleration with $g \approx 9.81\ \frac{\text{m}}{\text{s}^2}$.

$$P_{\text{pump}} = \frac{Q \cdot \rho}{\eta_{\text{pump}}} \cdot g \cdot \Delta h_{\text{geo}} + \frac{Q}{\eta_{\text{pump}}} \cdot \Delta p_{\text{L}} \qquad [P_{\text{pump}}] = \frac{\text{kWh}}{\text{d}} \tag{7.30}$$

The pressure loss Δp_{L} in the pipe, with diameter d_{pipe} and length l_{pipe}, is calculated using the Darcy-Weisbach equation

$$\Delta p_{\text{L}} = \frac{\lambda_{\text{pipe}} \cdot \rho \cdot {v_{\text{pipe}}}^2 \cdot l_{\text{pipe}}}{2 \cdot d_{\text{pipe}}} \qquad [\Delta p_{\text{L}}] = \text{Pa}. \tag{7.31}$$

The velocity of the medium in the pipe v_{pipe} is defined in equation (7.32) (Gerber, 2009).

$$v_{\text{pipe}} := \frac{4 \cdot Q}{\pi \cdot {d_{\text{pipe}}}^2} \qquad [v_{\text{pipe}}] = \frac{\text{m}}{\text{d}} \tag{7.32}$$

The calculation of the pressure loss coefficient λ_{pipe}, $[\lambda_{\text{pipe}}] = 100\ \%$, depends on the Reynolds number Re_{pipe}, which for a stream in a pipe is defined in equation (7.33) using the effective viscosity of the medium in the pipe $\eta_{\text{eff,pipe}}$, eq. (7.35) (Gerber, 2009).

$$Re_{\text{pipe}} := \frac{v_{\text{pipe}} \cdot d_{\text{pipe}} \cdot \rho}{\eta_{\text{eff,pipe}}} \qquad [Re_{\text{pipe}}] = 100\ \% \tag{7.33}$$

Using definition (7.33) and introducing the pipe roughness k_{pipe}, $[k_{\text{pipe}}] = \text{mm}$, the

pressure loss coefficient λ_{pipe} can be calculated in equation (7.34) (Türk, 1994).

$$\lambda_{\text{pipe}} \approx \begin{cases} \frac{64}{Re_{\text{pipe}}} & Re_{\text{pipe}} \leq 2300 \\ \frac{0.25}{\left[\log_{10}\left(\frac{15}{Re_{\text{pipe}}} + 0.2692 \cdot \frac{k_{\text{pipe}}}{d_{\text{pipe}}}\right)\right]^2} & 2300 < Re_{\text{pipe}} < 10^3 \cdot \frac{d_{\text{pipe}}}{k_{\text{pipe}}} \\ \frac{0.25}{\left[\log_{10}\left(3.715 \cdot \frac{d_{\text{pipe}}}{k_{\text{pipe}}}\right)\right]^2} & Re_{\text{pipe}} \geq 10^3 \cdot \frac{d_{\text{pipe}}}{k_{\text{pipe}}} \end{cases} \tag{7.34}$$

The effective viscosity of the medium in the pipe $\eta_{\text{eff,pipe}}$, $[\eta_{\text{eff,pipe}}] = \text{Pa} \cdot \text{s}$, is approximated using equation (7.35) (Türk, 1994), $[\text{TS}] \stackrel{!}{=} \%_{\text{FM}}, [\dot{\gamma}] \stackrel{!}{=} \text{s}^{-1}$.

$$\eta_{\text{eff,pipe}} \approx \begin{cases} \eta_{\text{w}} + C_{\text{visc}} \cdot \{\text{TS}\} & \text{TS} < 3\ \%_{\text{FM}} \\ K_{\text{c}} \cdot \left(\frac{3 \cdot n_{\text{flow}} + 1}{4 \cdot n_{\text{flow}}}\right)^{n_{\text{flow}}} \cdot \{\dot{\gamma}\}^{n_{\text{flow}} - 1} & 3\ \%_{\text{FM}} \leq \text{TS} \leq 8\ \%_{\text{FM}} \\ \frac{4 \cdot \tau_{\text{pipe}}}{\pi \cdot \dot{\gamma}} + K_{\text{c}} \cdot \left(\frac{\pi}{4} \cdot \{\dot{\gamma}\}\right)^{n_{\text{flow}} - 1} & \text{TS} > 8\ \%_{\text{FM}} \end{cases} \tag{7.35}$$

The viscosity of water η_{w}, $[\eta_{\text{w}}] = \text{Pa} \cdot \text{s}$, is calculated as in Gerber (2009) using a polynom of fifth order, shear rate $\dot{\gamma}$ and shear stress τ_{pipe} are given in equation (7.36) and (7.37), respectively.

$$\dot{\gamma} := \frac{8 \cdot v_{\text{pipe}}}{d_{\text{pipe}}} \stackrel{(7.32)}{=} \frac{32 \cdot Q}{\pi \cdot {d_{\text{pipe}}}^3} \qquad [\dot{\gamma}] = \frac{1}{\text{s}} \tag{7.36}$$

$$\tau_{\text{pipe}} := C_{\tau,1} \cdot \exp\left(C_{\tau,2} \cdot \{\text{TS}\}\right) \qquad [\tau_{\text{pipe}}] = \text{Pa}, \quad [\text{TS}] \stackrel{!}{=} \%_{\text{FM}} \tag{7.37}$$

The equations to calculate K_{c} and n_{flow} are (7.23) and (7.24), respectively. Parameter values for C_{visc}, $C_{K_{\text{c}},1}$, $C_{K_{\text{c}},2}$, $C_{n_{\text{flow}},1}$, $C_{n_{\text{flow}},2}$, $C_{\tau,1}$ and $C_{\tau,2}$ for different substrates can be found in Türk (1994) and Gerber (2009).

Solids Supply The power P_{solids} needed to feed the biogas plant with solid substrates is calculated in equation (7.38) using the specific energy value p_{char} given in $\frac{\text{kWh}}{\text{t}}$, the volumetric flow rate of the solid substrates Q_{IN} and the density of the substrates ρ_{IN}, eq. (7.7).

$$P_{\text{solids}} = p_{\text{char}} \cdot Q_{\text{IN}} \cdot \rho_{\text{IN}} \qquad [P_{\text{solids}}] = \frac{\text{kWh}}{\text{d}} \tag{7.38}$$

Values for the specific energy value p_{char} for typical solid supply units are given in Gerber (2009).

7.3.1.5 Heat Flux due to Substrate Feed

The volumetric flow rate of the substrate feed Q_{IN} with a temperature T_{IN} introduces a heat sink or source, depending on the digesters temperature T. In this thesis the simple approach, e.g. taken in Lübken et al. (2007b), is used to calculate the needed

(i.e. $T > T_{\mathrm{IN}}$, respectively released) power $P_{\mathrm{substrate}}$ in equation (7.39).

$$P_{\mathrm{substrate}} = Q_{\mathrm{IN}} \cdot \rho_{\mathrm{IN}} \cdot c_{\mathrm{substrate}} \cdot (T - T_{\mathrm{IN}}) \qquad [P_{\mathrm{substrate}}] = \frac{\mathrm{kWh}}{\mathrm{d}} \qquad (7.39)$$

The specific heat capacity of the substrates $c_{\mathrm{substrate}}$ is calculated as in Gerber (2009), whose approach is of the same type as in eq. (7.7), $[c_{\mathrm{substrate}}] = \frac{\mathrm{kJ}}{\mathrm{kg \cdot K}}$.
A more detailed approach is taken in Gerber (2009), which also incorporates the heat flux induced by the produced biogas and digestate leaving the digester.

7.3.1.6 Heat Loss through Digester Wall, Roof and Ground

The heat loss through the digester wall, roof and ground is calculated using three separate equations. The approach is similar to the approaches of Lindorfer et al. (2006), Lübken et al. (2007b) and the complex one in Gerber (2009). The radiation of the heat through the digester wall P_{wall} is calculated in equation (7.40) with the surface area of the cylindrical digester $A_{\mathrm{wall}} = \pi \cdot d_{\mathrm{dig}} \cdot h_{\mathrm{dig}}$. Here d_{dig} and h_{dig} are the digester diameter and wall height, respectively, see Fig. 7.5.

$$P_{\mathrm{wall}} = A_{\mathrm{wall}} \cdot k_{\mathrm{wall}} \cdot (T - T_{\mathrm{ambient}}) \qquad [P_{\mathrm{wall}}] = \frac{\mathrm{kWh}}{\mathrm{d}} \qquad (7.40)$$

In equation (7.40) the heat transfer coefficient of the wall k_{wall} and the ambient temperature T_{ambient} are used.

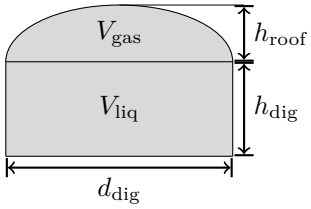

Figure 7.5: Schematic of a typical agricultural digester. h_{dig} and h_{roof} can be calculated using equations $V_{\mathrm{liq}} = \pi \cdot \frac{{d_{\mathrm{dig}}}^2}{4} \cdot h_{\mathrm{dig}}$ and $V_{\mathrm{gas}} = \frac{\pi}{6} \cdot h_{\mathrm{roof}} \cdot \left(\frac{3}{4}{d_{\mathrm{dig}}}^2 + {h_{\mathrm{roof}}}^2\right)$, respectively.

The heat loss through the roof P_{roof} is calculated in equation (7.41), assuming a roof surface $A_{\mathrm{roof}} = \pi \cdot \left(\frac{{d_{\mathrm{dig}}}^2}{4} + h_{\mathrm{roof}}^2\right)$ (see Fig. 7.5) and the heat transfer coefficient of the roof k_{roof}.

$$P_{\mathrm{roof}} = A_{\mathrm{roof}} \cdot k_{\mathrm{roof}} \cdot (T - T_{\mathrm{ambient}}) \qquad [P_{\mathrm{roof}}] = \frac{\mathrm{kWh}}{\mathrm{d}} \qquad (7.41)$$

The heat loss through the ground P_{ground} is calculated in equation (7.42) with the ground surface $A_{\mathrm{ground}} = \pi \cdot \frac{{d_{\mathrm{dig}}}^2}{4}$, the heat transfer coefficient of the ground k_{ground} and the ground temperature T_{ground}.

$$P_{\mathrm{ground}} = A_{\mathrm{ground}} \cdot k_{\mathrm{ground}} \cdot (T - T_{\mathrm{ground}}) \qquad [P_{\mathrm{ground}}] = \frac{\mathrm{kWh}}{\mathrm{d}} \qquad (7.42)$$

Values for all heat transfer coefficients, measured in $\frac{\mathrm{W}}{\mathrm{m^2 \cdot K}}$, can be found in Gerber (2009).

7.3.1.7 Thermal Energy Production due to Microbial Activity

The thermal energy production $P_{\mathrm{mic\_heat}}$ due to microbial activity inside the anaerobic digester is calculated in equation (7.43) using the parameters in Tables 7.4 and 7.5, Lübken et al. (2007b).

$$P_{\mathrm{mic\_heat}} = \sum_{j=5}^{12} \Delta E_j \cdot f_j \cdot \rho_j \cdot V_{\mathrm{liq}} \qquad [P_{\mathrm{mic\_heat}}] = \frac{\mathrm{kWh}}{\mathrm{d}} \tag{7.43}$$

Table 7.4: Calculation of thermal energy production due to microbial activity

Symbol	Description	Unit
f_j^{-1}	$\mathrm{g_{COD}}$ of 1 mol of the educt of process j	$\frac{\mathrm{g_{COD}}}{\mathrm{mol}}$
ρ_j	kinetic rate of process j of ADM1, Section 7.1	$\frac{\mathrm{kg_{COD}}}{\mathrm{m^3 \cdot d}}$
V_{liq}	digester volume of liquid phase	$\mathrm{m^3}$

Table 7.5: Values for energy released due to microbial activity ΔE_j (Lübken et al., 2007b)

j	Process	released energy ΔE_j, $[\Delta E_j] = \frac{\mathrm{kJ}}{\mathrm{mol}}$
5	uptake of sugars	−117.36
6	uptake of amino acids	−36.46
7	uptake of LCFA	494.88
8	uptake of valerate	89.99
9	uptake of butyrate	83.67
10	uptake of propionate	90.87
11	uptake of acetate	−27.34
12	uptake of hydrogen	−18.86

7.3.1.8 Others

The heat energy released to the digester by biological desulphurisation to reduce hydrogen sulphide in the gas phase by addition of fresh air is calculated in Lindorfer et al. (2006). Furthermore, oxygen, reacting in an exothermic reaction, is also fed to the digester together with the solid substrates, which is modeled in Lindorfer et al. (2006) as well. In Gebremedhin et al. (2005) solar radiation and in Wu and Bibeau (2006) a 3-d heat transfer model for an anaerobic digester are developed. Axaopoulos et al. (2001) combines solar collectors with an anaerobic digester.

7.3.1.9 Summary

To summarize the energy part 7.3.1 now follows what is done with the produced and consumed energy values.

The produced electrical energy per day P_{el} (eq. (7.17)) is injected into the local electricity grid, which is benefited financially on a kWh basis, see the next section on finance Section 7.3.2.

The consumed electrical energy per day

$$P_{\mathrm{el,consume}} := P_{\mathrm{MIX}} + P_{\mathrm{pump}} + P_{\mathrm{solids}} \qquad [P_{\mathrm{el,consume}}] = \frac{\mathrm{kWh}}{\mathrm{d}} \tag{7.44}$$

must be bought from the local energy provider (eqs. (7.28), (7.30) and (7.38)).

The daily thermal energy balance of a biogas plant ΔP_{th}, $[\Delta P_{\mathrm{th}}] = \frac{\mathrm{kWh}}{\mathrm{d}}$, is calculated as follows (using eqs. (7.18), (7.29), (7.39), (7.40), (7.41), (7.42) and (7.43))

$$\Delta P_{\mathrm{th}} := P_{\mathrm{th}} + P_{\mathrm{diss}} + P_{\mathrm{mic\_heat}} - P_{\mathrm{substrate}} - (P_{\mathrm{wall}} + P_{\mathrm{roof}} + P_{\mathrm{ground}})\,. \tag{7.45}$$

If ΔP_{th} is negative, then the remaining thermal energy must be produced by a heating with an efficiency η_{heat}, $[\eta_{\mathrm{heat}}] = 100\ \%$. This is for example the case when the biogas plant has no CHP. If ΔP_{th} is positive, then the surplus thermal energy is assumed to be used externally for heating. This part of thermal energy gets either a real or a virtual financial value, such that it can be balanced with the financial value of the electrical energy and the substrate costs, see Section 7.3.2.

7.3.2 Finance

The profit obtained selling the produced electrical and thermal energy in Germany is determined by the Renewable Energy Sources Act - EEG, BMU (2012a). In the year 2000 the first version of the EEG came into force, with reissues in the years 2004, 2009 and 2012. Both EEG versions of 2009 and 2012 are implemented in the developed MATLAB® toolbox, see appendix Part B. They both have in common, that a basic remuneration for each produced kWh electric is paid. The value of the remuneration depends on the total electrical power of the plant and the year of construction. On top of the basic remuneration further payments are possible, which depend on criteria the biogas plant has to meet.

EEG 2009 In the EEG 2009 a bonus system defines the additional remuneration. The payment per electrical kWh is for example increased if the produced thermal energy is used as well, substrates taken from the preservation of the countryside are used and if at least thirty mass percent of the substrate feed is manure (manure bonus). For each fulfilled bonus the total remuneration is increased.

EEG 2012 In the EEG 2012 all bonuses were dropped, except for the bonus of gas preparation, which existed already in the EEG 2009. Instead of the bonuses, the additional remuneration became dependent on the fed substrates directly. All possible substrates are classified into three categories, whereas the categories are remunerated differently. If substrates from different substrate classes are used, then the proportionally produced amount of methane of each substrate defines the height of the remuneration. The EEG 2012 defines as precursor a minimal thermal energy usage of 35 %.

Profit The total profit of the produced electrical and thermal energy E_{plant}, $[E_{\text{plant}}] = €$, is calculated in the following simplified manner. The remuneration for the produced electrical energy (as calculated in EEG 2009 or 2012) is symbolized by r_{EEG} and costs for electrical energy by p_{el}, $[r_{\text{EEG}}] = [p_{\text{el}}] = \frac{€}{\text{kWh}_{\text{el}}}$. The virtual or real revenue of the produced thermal energy is denoted by r_{th}. If thermal energy is consumed instead, thus $\Delta P_{\text{th}} < 0$, the costs for producing the needed thermal energy shall be given by p_{th}, $[r_{\text{th}}] = [p_{\text{th}}] = \frac{€}{\text{kWh}_{\text{th}}}$. In the toolbox the financial profit is calculated as given in eq. (7.46) using eqs. (7.17), (7.44) and (7.45).

$$E_{\text{plant}} := \begin{cases} P_{\text{el}} \cdot r_{\text{EEG}} - P_{\text{el,consume}} \cdot p_{\text{el}} + \Delta P_{\text{th}} \cdot r_{\text{th}} - p_{\text{IN}} & \Delta P_{\text{th}} \geq 0 \\ P_{\text{el}} \cdot r_{\text{EEG}} - P_{\text{el,consume}} \cdot p_{\text{el}} + \Delta P_{\text{th}} \cdot \eta_{\text{heat}} \cdot p_{\text{th}} - p_{\text{IN}} & \Delta P_{\text{th}} < 0 \end{cases} \tag{7.46}$$

If more than one substrate is fed to the biogas plant the total substrate costs is a sum over all single substrate costs p_{IN} and has to be inserted in the equation instead. In the calculation of the profit all other costs such as man hours, credit rates, etc. are neglected, because they are seen as fix costs, which are independent of the substrate feed.

Although not explicitly stated, the profit E_{plant} is a function of the plant's state and substrate feed. So, in mathematical terms, $E_{\text{plant}} : \mathcal{X} \times \mathcal{U} \to \mathbb{R}$. The reason is, that e.g. the produced electrical power P_{el} depends on the state of the biogas plant, because the produced biogas Q_{gas} does (see eqs. (7.3) and (7.17)). Furthermore, the substrate costs p_{IN} are directly linked to the substrate feed. The profit E_{plant} is used in the definition of the objective function in Section 7.3.4.

7.3.3 Physics and Chemistry

7.3.3.1 COD Degradation Rate

The degradation rate of the COD, which is fed with the substrate (see Section 7.2), is a criteria used in the objective function. Both, total soluble COD and total particulate COD are investigated.

The total soluble COD concentration $\mathrm{SS_{COD,IN}}$ fed to the digester is defined in equation (7.47). The components of the input vector ${}^{o}\boldsymbol{u}_{\mathrm{AD}} := ({}^{o}u_{\mathrm{AD},1}, \ldots, {}^{o}u_{\mathrm{AD},i}, \ldots, {}^{o}u_{\mathrm{AD},34})^{T}$ are defined in equation (7.2).

$$\mathrm{SS_{COD,IN}} := \sum_{i=1}^{9} {}^{o}u_{\mathrm{AD},i} + S_{\mathrm{I,IN}} \qquad [\mathrm{SS_{COD,IN}}] = \frac{\mathrm{kg_{COD}}}{\mathrm{m^3}} \tag{7.47}$$

The total soluble COD concentration flowing out of the digester and into the final storage tank is symbolized by $\mathrm{SS_{COD,FST}}$, defined in equation (7.48) using the ADM1 state variables defined in eq. (7.2).

$$\mathrm{SS_{COD,FST}} := \sum_{i=1}^{9} {}^{o}x_{\mathrm{AD},i} + S_{\mathrm{I}} \qquad [\mathrm{SS_{COD,FST}}] = \frac{\mathrm{kg_{COD}}}{\mathrm{m^3}} \tag{7.48}$$

The degradation rate of soluble COD is defined in equation (7.49) using the volumetric flow rate of the substrate feed Q_{IN} and the volumetric flow rate of the sludge flowing into the final storage tank Q_{FST}, both measured in $\frac{\mathrm{m^3}}{\mathrm{d}}$.

$$\mathrm{COD_{SS,degrade}} := \frac{\mathrm{SS_{COD,FST}} \cdot Q_{\mathrm{FST}}}{\mathrm{SS_{COD,IN}} \cdot Q_{\mathrm{IN}}} \in [0,1] \tag{7.49}$$

The total particulate COD of the substrate feed $\mathrm{VS_{COD,IN}}$ is defined in eq. (7.50) and the particulate COD leaving the digester $\mathrm{VS_{COD,FST}}$ is defined in eq. (7.51).

$$\mathrm{VS_{COD,IN}} := \sum_{i=13}^{25} {}^{o}u_{\mathrm{AD},i} \qquad [\mathrm{VS_{COD,IN}}] = \frac{\mathrm{kg_{COD}}}{\mathrm{m^3}} \tag{7.50}$$

$$\mathrm{VS_{COD,FST}} := \sum_{i=13}^{25} {}^{o}x_{\mathrm{AD},i} \qquad [\mathrm{VS_{COD,FST}}] = \frac{\mathrm{kg_{COD}}}{\mathrm{m^3}} \tag{7.51}$$

Again, the degradation rate of total particulate COD is defined in equation (7.52).

$$\mathrm{COD_{VS,degrade}} := \frac{\mathrm{VS_{COD,FST}} \cdot Q_{\mathrm{FST}}}{\mathrm{VS_{COD,IN}} \cdot Q_{\mathrm{IN}}} \in [0,1] \tag{7.52}$$

7.3.3.2 Faecal Bacteria Removal Capacity

In Lübken (2009), Lübken et al. (2007a) the removal capacity of anaerobic digestion for faecal bacteria is studied. Two models for two bacteria are proposed using multiple regression. In eq. (7.53) the removal capacity for intestinal enterococci η_{IE} and in eq. (7.54) the one for faecal coliforms η_{FC} is given.

$$\eta_{\mathrm{IE}} = 98.29 - 2.2 \cdot \left(\frac{1}{\{\mathrm{HRT}\}}\right)^{2} + 0.031 \cdot \{T\} \qquad [\eta_{\mathrm{IE}}] = \% \tag{7.53}$$

$$\eta_{\mathrm{FC}} = 98.29 - 1.0 \cdot \left(\frac{1}{\{\mathrm{HRT}\}}\right)^{2} + 0.031 \cdot \{T\} \qquad [\eta_{\mathrm{FC}}] = \% \tag{7.54}$$

As parameters the digester temperature T, $[T] \stackrel{!}{=} {}^{o}\mathrm{C}$, and the hydraulic retention time HRT, $[\mathrm{HRT}] \stackrel{!}{=} \mathrm{d}$, are used.

7.3.3.3 The pH Value

The pH value is defined as the negative value of the common logarithm of the activity of hydrogen ions (Nielsen et al., 2008). Nevertheless, in ADM1 it is assumed, that the ion activity can be approximated with the concentration of the hydrogen ion $c\left(\mathrm{H}^{+}\right)$, thus pH is calculated as:

$$\mathrm{pH} \approx -\log_{10}\left(c\left(\mathrm{H}^{+}\right)\right).$$

For a discussion on the validity of this assumption see Nielsen et al. (2008). Inside the digester (likewise in the substrate) the concentration of the hydrogen ion is calculated in equation (7.55) using the dissociation constant of water $K_{\mathrm{w}} \in \mathbb{R}^{+}$ and the total alkalinity value TA defined in eq. (7.61) (Tschepetzki and Ogurek, 2010). To calculate the pH value of the substrate the values $\mathrm{TA}_{\mathrm{IN}}$ and $S^{+}_{\mathrm{nh4,IN}}$ are used instead of TA and S^{+}_{nh4}, respectively; $[\mathrm{TA}] \stackrel{!}{=} \left[S^{+}_{\mathrm{nh4}}\right] \stackrel{!}{=} \frac{\mathrm{mol}}{\mathrm{l}}$.

$$c\left(\mathrm{H}^{+}\right) = \frac{\{\mathrm{TA}\} - \left\{S^{+}_{\mathrm{nh4}}\right\} + \sqrt{\left(-\{\mathrm{TA}\} + \left\{S^{+}_{\mathrm{nh4}}\right\}\right)^{2} + 4 \cdot K_{\mathrm{w}}}}{2} \tag{7.55}$$

7.3.3.4 Propionic to Acetic Acid Concentration

There are indications, that the ratio of propionic to acetic acid in the digester is a good indicator to determine process instability (Hill et al., 1987, Marchaim and Krause, 1993). But there are also results that show that it is possible to have a stable process with high values of that ratio (Ahring et al., 1995, Pullammanappallil et al., 2001). Nevertheless, this criterion is included in the model and implemented as:

$$P/A := \frac{S_{\mathrm{pro}}}{S_{\mathrm{ac}}} \qquad [S_{\mathrm{pro}}] \stackrel{!}{=} [S_{\mathrm{ac}}] \stackrel{!}{=} \frac{\mathrm{mol}}{\mathrm{l}} \tag{7.56}$$

7.3.3.5 Total Solids in Digester

Given the relation between the TS content $\mathrm{TS}_{\mathrm{IN}}$ and the particulate chemical oxygen demand $\mathrm{COD}_{\mathrm{X}}$ of a substrate in equation (7.6) the total solids content TS in the digester is approximated using equation (7.57). For the description of all parameters see Section 7.2.

$$\mathrm{TS} \approx \mathrm{ash} + \frac{\mathrm{VS}_{\mathrm{IN}}}{\rho_{\mathrm{IN}}} \cdot \frac{1}{\mathrm{VS}_{\mathrm{IN}} \cdot \overline{\mathrm{ThOD}}} \cdot \underbrace{\sum_{i=13}^{25} {}^{o}x_{\mathrm{AD},i}}_{\stackrel{(7.51)}{=} \mathrm{VS}_{\mathrm{COD,FST}}} \qquad [\mathrm{TS}] = \%_{\mathrm{FM}} \tag{7.57}$$

As for the estimation of the TS inside the digester substrate parameters are used, this clearly is only an approximation. To avoid confusion it should be claimed, that here the particulate COD inside the digester and not inside the final storage tank must be used. For the plant configuration assumed here, consisting out of only one digester, both values are the same.

7.3.3.6 Volatile Solids in Digester

The volatile solids content VS inside a digester is calculated out of the estimated TS content in the digester (see above, eq. (7.57)) and the ash content of the substrate feed. Assuming that the ash content inside the digester is the same as the one of the substrate feed, the volatile solids content VS inside the digester is given as in equation (7.58).

$$\{\mathrm{VS}\} := 1 - \frac{\{\mathrm{ash}\}}{\{\mathrm{TS}\}} \qquad [\mathrm{ash}] \stackrel{!}{=} [\mathrm{TS}] \stackrel{!}{=} \%_{\mathrm{FM}}, \qquad [\mathrm{VS}] = 100\ \%_{\mathrm{TS}} \tag{7.58}$$

7.3.3.7 Volatile Solids Degradation Rate

The degradation rate of volatile solids during anaerobic digestion is calculated in equation (7.59), Koch (2010).

$$\mathrm{VS}_{\mathrm{degrade}} := 1 - \frac{\mathrm{VS}_{\mathrm{FST}} \cdot (1 - \{\mathrm{VS}_{\mathrm{IN}}\})}{(1 - \{\mathrm{VS}_{\mathrm{FST}}\}) \cdot \mathrm{VS}_{\mathrm{IN}}} \in [0, 1] \qquad [\mathrm{VS}_{\mathrm{IN}}] \stackrel{!}{=} [\mathrm{VS}_{\mathrm{FST}}] \stackrel{!}{=} 100\ \%_{\mathrm{TS}} \tag{7.59}$$

The volatile solids content of the substrate feed $\mathrm{VS}_{\mathrm{IN}}$ is measured in 100 $\%_{\mathrm{TS}}$ as well as the volatile solids content entering the final storage tank $\mathrm{VS}_{\mathrm{FST}}$. In this scenario the latter is equal to the volatile solids content inside the digester as calculated in eq. (7.58).

7.3.3.8 VFA/TA Value

As proposed in Schoen et al. (2009) the VFA/TA value is modeled using the volatile fatty acids concentration VFA calculated in equation (7.60)

$$\mathrm{VFA} := S_{\mathrm{ac}} + S_{\mathrm{pro}} + S_{\mathrm{bu}} + S_{\mathrm{va}} \qquad [\mathrm{VFA}] = \frac{\mathrm{gHAceq}}{\mathrm{l}} \tag{7.60}$$

and the total alkalinity value TA as calculated in eq. (7.61). The process values used in both calculations are defined in Table 7.1.

$$\mathrm{TA} := S_{\mathrm{an}}^{-} + S_{\mathrm{hco3}}^{-} + S_{\mathrm{ac}}^{-} + S_{\mathrm{pro}}^{-} + S_{\mathrm{bu}}^{-} + S_{\mathrm{va}}^{-} - S_{\mathrm{cat}}^{+} \qquad [\mathrm{TA}] = \frac{\mathrm{gCaCO_3eq}}{\mathrm{l}} \tag{7.61}$$

The $\mathrm{VFA/TA} := \frac{\mathrm{VFA}}{\mathrm{TA}}$ is measured in $\frac{\mathrm{gHAceq}}{\mathrm{gCaCO_3eq}}$. The VFA/TA value is an important stability indicator for a biogas plant, which should be around $(0.15 - 0.45)\ \frac{\mathrm{gHAceq}}{\mathrm{gCaCO_3eq}}$ (Voßet al., 2009).

7.3.4 Objective Function

The objective function, once defined in equation (2.13), in this thesis is implemented as a two-dimensional function: $\boldsymbol{J} := (J_1, J_2)^T$, thus the number of objectives is $n_\mathrm{o} = 2$. The objective function $\boldsymbol{J}$ contains out of an integral over the stage cost $\boldsymbol{F} := (F_1, F_2)^T$ plus a terminal cost (also called terminal penalty term) $\boldsymbol{T}_\mathrm{penalty} := (T_{\mathrm{penalty},1}, T_{\mathrm{penalty},2})^T$, e.g. see eq. (7.62).
The first component of the objective function J_1,

$$J_1 := \frac{1}{T_\mathrm{p}} \cdot \int_{t_k}^{t_k+T_\mathrm{p}} F_1(\tau)\ \mathrm{d}\tau + T_{\mathrm{penalty},1}, \tag{7.62}$$

is defined as the average of the negative financial profit E_plant (defined in eq. (7.46)) obtained by operating the biogas plant over the prediction horizon T_p, with

$$F_1(\tau) := -E_\mathrm{plant}\left({}^o\boldsymbol{x}(\tau), {}^o\boldsymbol{u}(\tau)\right) \qquad [F_1] = \frac{€}{1000}. \tag{7.63}$$

The minus sign in eq. (7.63) is added because the optimization problem in eq. (2.18) is formulated as a minimization problem. In eq. (7.62) the first component of the terminal cost $T_{\mathrm{penalty},1}$ is used, which is defined as:

$$T_{\mathrm{penalty},1} := \kappa_{T,1} \cdot F_1\left(t_k + T_\mathrm{p}\right), \tag{7.64}$$

with the weighting factor $\kappa_{T,1} \in \mathbb{R}^+$.
The second component of the objective function J_2,

$$J_2 := \frac{1}{T_\mathrm{p}} \cdot \int_{t_k}^{t_k+T_\mathrm{p}} F_2(\tau)\ \mathrm{d}\tau + \int_{t_k}^{t_k+T_\mathrm{p}} \left\| {}^o\boldsymbol{u}'(\tau) \right\|_2^2\ \mathrm{d}\tau + T_{\mathrm{penalty},2}, \tag{7.65}$$

contains a weighted sum of all $n_\mathrm{c} \in \mathbb{N}_0$ constraints that are active over the prediction horizon, defined in the second component of the stage cost F_2:

$$F_2(\tau) := \sum_{i_\mathrm{c}=1}^{n_\mathrm{c}} \kappa_{i_\mathrm{c}} \cdot \mathrm{constraint}_{i_\mathrm{c}}\left({}^o\boldsymbol{x}(\tau), {}^o\boldsymbol{u}(\tau)\right) \qquad [F_2] = 1. \tag{7.66}$$

Furthermore J_2 contains the integral over the change of the open loop control input ${}^o\boldsymbol{u}$ and the terminal penalty term $T_{\mathrm{penalty},2}$ with the weighting factor $\kappa_{T,2} \in \mathbb{R}^+$:

$$T_{\mathrm{penalty},2} := \kappa_{T,2} \cdot F_2\left(t_k + T_\mathrm{p}\right) \tag{7.67}$$

In eq. (7.66) the weights $\kappa_{i_\mathrm{c}} \in \mathbb{R}^+$ are normalized, $\sum_{i_\mathrm{c}}^{n_\mathrm{c}} \kappa_{i_\mathrm{c}} = 1$, and the constraints are defined as:

$$\mathrm{constraint}_{i_\mathrm{c}} : \mathcal{X} \times \mathcal{U} \to \begin{cases} 0 & \text{if inactive} \\ 0 < \cdots \leq 1 \text{ or } \frac{4.6851^2}{6} & \text{if active.} \end{cases} \tag{7.68}$$

Such that all constraints are smooth, some of the them are implemented using the Tukey biweight function $\rho_\mathrm{Ty} : \mathbb{R} \to \mathbb{R}^+$, which is defined as, with $C_\mathrm{Ty} := 4.6851$

(Comport et al., 2006):

$$\rho_{\mathrm{Ty}}\left(u_{\mathrm{Ty}}\right) := \begin{cases} \frac{C_{\mathrm{Ty}}^2}{6}\left[1-\left(1-\left(\frac{u_{\mathrm{Ty}}}{C_{\mathrm{Ty}}}\right)^2\right)^3\right] & |u_{\mathrm{Ty}}| \leq C_{\mathrm{Ty}} \\ \frac{C_{\mathrm{Ty}}^2}{6} & \text{else.} \end{cases} \tag{7.69}$$

In eq. (7.69) $u_{\mathrm{Ty}} \in \mathbb{R}$ must be replaced by the difference between the constrained value and its constraint. An alternative to Tukey's biweight function could be to use Harrington's desirability function (Wagner and Trautmann, 2010). For all entries mentioned in Section 7.3.3 there exist one or two constraint definitions. The following list gives an overview:

- COD degradation rate: eqs. (7.49) and (7.52) are normalized soft constraints
- Faecal Bacteria Removal Capacity: using eqs. (7.53) and (7.54) normalized soft constraints can be stated
- pH value: lower and upper boundary as normalized hard constraint
- propionic to acetic acid concentration: upper boundary for equation (7.56) using equation (7.69)
- total solids in digester: upper boundary for eq. (7.57) using eq. (7.69)
- volatile solids degradation rate: lower boundary for equation (7.59) (not yet implemented)
- VFA/TA value: upper boundary using eq. (7.69)
- VFA: lower and upper boundary for eq. (7.60) using eq. (7.69)
- TA: lower boundary for eq. (7.61) using eq. (7.69)
- OLR: upper boundary for eq. (5.9) using eq. (7.69)
- HRT: lower and upper boundary for eq. (5.7) using eq. (7.69)
- sum of ammonia S_{nh3} and ammonium S_{nh4}^{+}: upper boundary using eq. (7.69)
- methane concentration in biogas: lower boundary using eq. (7.69)
- excess biogas: lost profit in 1000 €/d
- degree of utilization of CHPs: normalized soft constraint

As defined in eq. (2.19) the optimal substrate feed is determined by the minimum value of the scalar objective function, which is also called fitness,

$$J_{1\mathrm{D}} := \sum_{i_{\mathrm{o}}=1}^{n_{\mathrm{o}}} \varpi_{i_{\mathrm{o}}} \cdot J_{i_{\mathrm{o}}} \overset{n_{\mathrm{o}}=2}{=} \varpi_1 \cdot J_1 + \varpi_2 \cdot J_2. \tag{7.70}$$

In Chapter 9 also the one-dimensional stage cost $F_{1\mathrm{D}}$ will be needed:

$$F_{1\mathrm{D}} := \sum_{i_{\mathrm{o}}=1}^{n_{\mathrm{o}}} \varpi_{i_{\mathrm{o}}} \cdot F_{i_{\mathrm{o}}} \overset{n_{\mathrm{o}}=2}{=} \varpi_1 \cdot F_1 + \varpi_2 \cdot F_2. \tag{7.71}$$

In this thesis ecological criteria are not yet integrated in the objective function. Ecology of biogas plants is discussed in life cycle assessment (LCA), see e.g. (Berglund and

Börjesson, 2006, Cherubini and Strø mman, 2011, Patterson et al., 2011).

7.4 Model Implementation of an Agricultural Biogas Plant

In the simulation experiments performed in Chapter 8 and Chapter 9 a model of a biogas plant is used. This model and the real plant are described here. The modeled biogas plant is a full-scale agricultural biogas plant with an electrical power of 500 kW, located in Germany. The plant is configured as a two-stage system with a primary (1st) ($V_{\text{liq}} = 1977$ m^3) and a secondary (or post) digester ($V_{\text{liq}} = 4182$ m^3), whereas the secondary digester also serves as final storage tank. A pumping station offers the possibility of interchanging sludge between both digesters. The first digester is mainly fed with maize silage, swine and cattle manure as well as varying substrates such as grass silage, corn-cob-mix (CCM) and whole crop silage (German: Ganzpflanzensilage - GPS). The secondary digester is not fed. The produced biogas is burned in two CHPs with an electrical power of 250 kW each. The produced power P_{el} is injected into the local grid, which is enumerated by the EEG 2009 (Section 7.3.2). Both digesters are heated with the thermal energy produced by the CHPs and are operated at about $T = 40$ ^{o}C in the mesophilic temperature region. The biogas plant is fed based on the observed vs. the expected biogas production, but in an open loop fashion. The main target is to run the CHPs at full capacity. The produced biogas is analyzed online by a gas analysator, which measures CH_4, CO_2 and H_2.

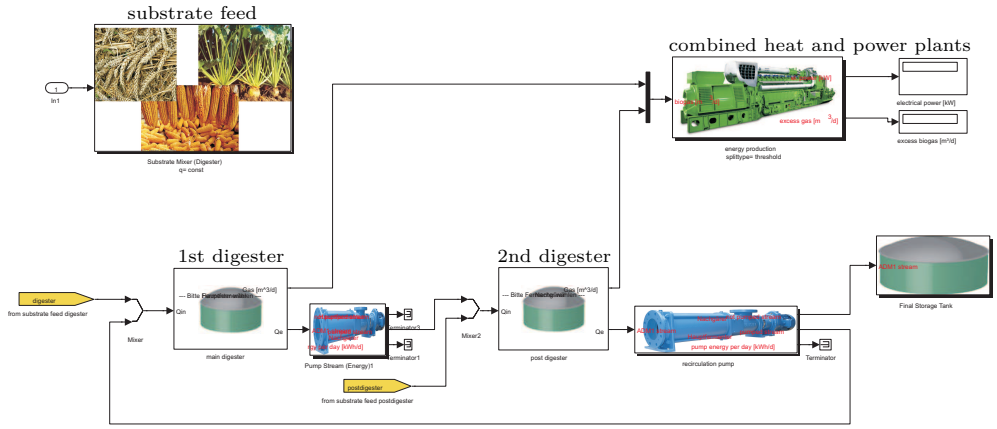

Figure 7.6: Model implementation of the agricultural biogas plant in Simulink®.

The simulation model is implemented in MATLAB® in a self-developed toolbox which is used for all performed simulation experiments in this thesis. For more details about the toolbox see Part B of the appendix. The implementation of the biogas plant model

is depicted in Figure 7.6. One can see the two digesters, two pumps, one block for mixing the substrates and a block representing the two combined heat and power plants. The secondary digester is implemented by two separate blocks: the post digester block and the final storage tank block. All aspects that were discussed in this chapter are implemented in this model.

7.5 Model Calibration and Validation

To achieve reliable simulation results for the modeled biogas plant the most sensitive parameters of the ADM1 have to be calibrated. However, (Ogurek and Alex, 2013) points out that before calibration of parameters the model structure should be checked. E.g., if a large CSTR reactor is modeled it might be very valuable to model this reactor with more than one CSTR model, which are stacked vertically to model different layers in the real digester. To reduce complexity and computation time, in this thesis only one CSTR is used to model the real digester.

Sensitivity analyses for the ADM1 have been performed a lot, e.g. Jeong et al. (2005), Lee et al. (2009), Wichern et al. (2008) and Wolfsberger (2008). Model calibration can be done manually or be stated as an optimization problem as is e.g. done in Wenzel (2008) and Wichern et al. (2009). For a review see Donoso-Bravo et al. (2011).

The above described biogas plant model is calibrated manually based on offline and online measurements. Due to a limited budget the cost intensive offline measurements could not be taken into account for the validation period as well, so that validation was only possible based on online measurements. The calibration period ran from 22/11/2011 until 22/01/2012 followed by the validation period until 21/04/2012. At that time the plant was fed with maize silage, swine manure and partly corn-cob-mix and grass silage, see Figure 7.7. The parameters of these four substrates as is defined in Table 7.3 are listed in Table 7.6. The given parameter values are either determined by repetitive measurement of different substrate probes or estimated by using typical values for each individual substrate.

Model calibration was based on model parameters which either were connected to the substrates or associated with the digesters. The disintegration rate k_{dis} and the maximum uptake rates $k_{\mathrm{m,c4}}, k_{\mathrm{m,pro}}, k_{\mathrm{m,ac}}$ and $k_{\mathrm{m,h2}}$ are modeled to be substrate dependent and the half saturation coefficient for ammonia $K_{\mathrm{I,NH3}}$ is linked to the digesters directly. All other ADM1 parameters are set to default values as given in Tschepetzki and Ogurek (2010), which can be found in Part C of the appendix. The maximum uptake rates were attached to the substrates because of their wide spectrum of values for an agricultural feedstock reported in the literature, e.g. Gehring et al. (2009), Girault et al. (2011), Koch et al. (2010), Wichern et al. (2007, 2008, 2009) and Wolfsberger (2008). Although a dependency of these parameters on the biogas plant's

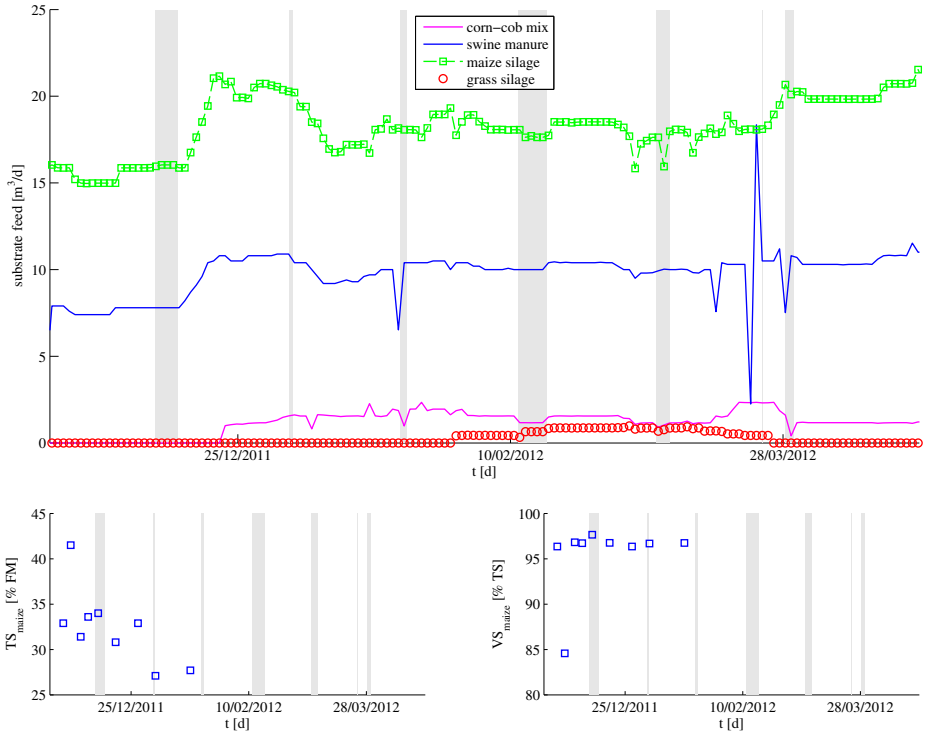

Figure 7.7: Top: Substrate feed of the full-scale biogas plant during calibration and validation. Bottom: Total solids (left) and volatile solids (right) of maize silage measured during the calibration period. Periods highlighted by the gray colored vertical bars symbolize times where no online data could be recorded.

state is more likely, without a model for this dependency the parameters can only be related to the substrates which on the other hand influence the digester's state. The calibrated values for the substrate dependent parameters are given in Table 7.7 and the value for the parameter $K_{\mathrm{I,NH3}}$ was set to 0.0020 $\frac{\mathrm{kmolN}}{\mathrm{m}^3}$ for the first digester and to 0.0011 $\frac{\mathrm{kmolN}}{\mathrm{m}^3}$ for the second digester (default: 0.0018 $\frac{\mathrm{kmolN}}{\mathrm{m}^3}$).

Calibration and validation results are depicted in Figure 7.8 for online measured variables and in Figure 7.9 for offline measured variables.

As can be seen in Figure 7.8 biogas and electrical energy production can be modeled quite reasonably. The reference signal for the biogas flow rate is not measured directly but calculated out of the differential of stored biogas in the gas chamber and consumed biogas in the CHPs. Therefore, the reference signal is quite noisy and error prone. The simulated electrical energy assumed a continuous operation of the CHPs. But, as can be seen in the reference signal of the electrical power, there are quite a lot of negative peaks in the data that signalize down times of either one of the two CHPs, e.g. due to maintenance.

Table 7.6: Measured parameters for substrate feed characterization.

parameter	maize silage	swine manure	corn-cob-mix	grass silage	unit
TS_{IN}	Fig. 7.7	6.1	67.6	34.1	$\%_{FM}$
VS_{IN}	Fig. 7.7	71.6	93.5	84.6	$\%_{TS}$
RP	8.69	16.31	10.54	17.5	$\%_{TS}$
RL	3.68	4.55	5.3	6.6	$\%_{TS}$
NDF	43.64	50.64	43.64	47.5	$\%_{TS}$
ADF	21.86	35.86	21.86	29.8	$\%_{TS}$
ADL	2.15	3.15	4.01	5.3	$\%_{TS}$
pH_{IN}	3.93	7.1	4.0	4.1	–
$S^{+}_{nh4,IN}$	0.66	4	0.55	1.5	$\frac{g}{l}$
TA_{IN}	6	212.22	5.69	7.01	$\frac{mmol}{l}$
T_{IN}	13	16.37	10	10	^{o}C
$S_{va,IN}$	0	0	0	0	$\frac{g}{l}$
$S_{bu,IN}$	0	0	0	0	$\frac{g}{l}$
$S_{pro,IN}$	0	0.8	0.6	0	$\frac{g}{l}$
$S_{ac,IN}$	1.18	12.43	3.5	1.53	$\frac{g}{l}$
D_{VS}	0.8	0.95	0.95	0.75	100 %
$k_{hyd,ch}$	10	10	10	10	$\frac{1}{d}$
$k_{hyd,pr}$	10	10	10	10	$\frac{1}{d}$
$k_{hyd,li}$	10	10	10	10	$\frac{1}{d}$
$COD_{filtrate}$	15.97	20	46.3	27.89	$\frac{kg_{COD}}{m^3}$
$S_{I,IN}$	13.03	7.3	35.3	22.89	$\frac{kg_{COD}}{m^3}$
p_{IN}	40	4	135	25	$\frac{€}{t}$

The measured methane content in the produced biogas is very noisy. Furthermore, the sensor seems not to be calibrated well. Although on 11/02/2012 the sensor was recalibrated, the simulated biogas and methane content shortly after that date cannot produce as much electrical power as was measured.

The level of hydrogen in the produced biogas can basically be modeled, but not their dynamics which often signalize process disturbances. E.g. the peak on 05/01/2012 was due to contaminated manure. As the contamination was not modeled the peak could not be represented in the simulation results.

The offline measured variables can essentially be modeled (see Figure 7.9). As the offline measurements are done in single probes taken out of the large digesters, it must be questioned whether the measured values are really of ground truth. Therefore, during calibration it is not tried to pay attention to each individual measurement, but more to

Table 7.7: Calibrated values of the substrate dependent ADM1 parameters. At the bottom of the table the default value (Tschepetzki and Ogurek, 2010) and a range of values found in the literature are given.

Substrate	k_{dis}	$k_{\mathrm{m,c4}}$	$k_{\mathrm{m,pro}}$	$k_{\mathrm{m,ac}}$	$k_{\mathrm{m,h2}}$
maize silage	0.14	20	3.8	4.8	35.9
swine manure	0.27	20	3.8	6.8	36.1
corn-cob mix	0.06	20	4	4.2	35.9
grass silage	0.04	20	8	4.9	35.6
default	0.5	20	13	8	35
range in literature	0.05 - 1.74	13.7 - 35	3.8 - 23.3	3.6 - 17.9	5 - 35

the general trend. In the beginning of the calibration period the VFA concentration in the post digester was quite high, even higher as in the first digester. This was due to the butyric acid concentration in the probe, which could not be modeled accurately in the beginning of the calibration period. The total alkalinity in the first digester was a little under-predicted and in the secondary digester a little over-predicted. Furthermore, the total solids content in the secondary digester is over-predicted. The measured pH values in both digesters are a bit higher as simulated.

In Figures 7.10 and 7.11 4-plot analyses (Fortuna et al., 2007) of the model residuals for biogas volumetric flow rate Q_{gas} and methane concentration $r_{\mathrm{ch_4}}$ are visualized. In the plots one can see whether the assumption is true that the obtained residuals are roughly normal, with a mean of 0 and some constant variance, and independently distributed[2]. In the top left of a 4-plot analysis a run sequence plot is shown. In the plot it can be observed whether a time dependency does exist. In the run sequence plot of Figure 7.10 a shift in the lowest frequency can be seen. In the beginning it is much higher as in the end. In Figure 7.11 from around sample 190 onwards a shift and slow drift in location can be observed. The shift comes with the recalibration of the sensor. If the lag plot, top right, is structureless, then the randomness assumption holds. Especially in Figure 7.10 the lag plot shows a slightly linear structure, thus the randomness assumption does not hold here. In the histogram, bottom left, the distribution of the residuals can be studied. In both figures a normal distribution may be assumed, where as the one in Figure 7.10 has a too long tail in the direction of high residual values. In the right bottom corner of a 4-plot analysis a normal probability plot is shown. If all residuals lie on the visualized line, then they are normally distributed. This is especially true for the residuals in Figure 7.11.

Based on the presented validation results it can be seen how difficult it is to calibrate such a complex model to a full-scale biogas plant. The quality, amount and domain

[2] `http://www.itl.nist.gov/div898/handbook`

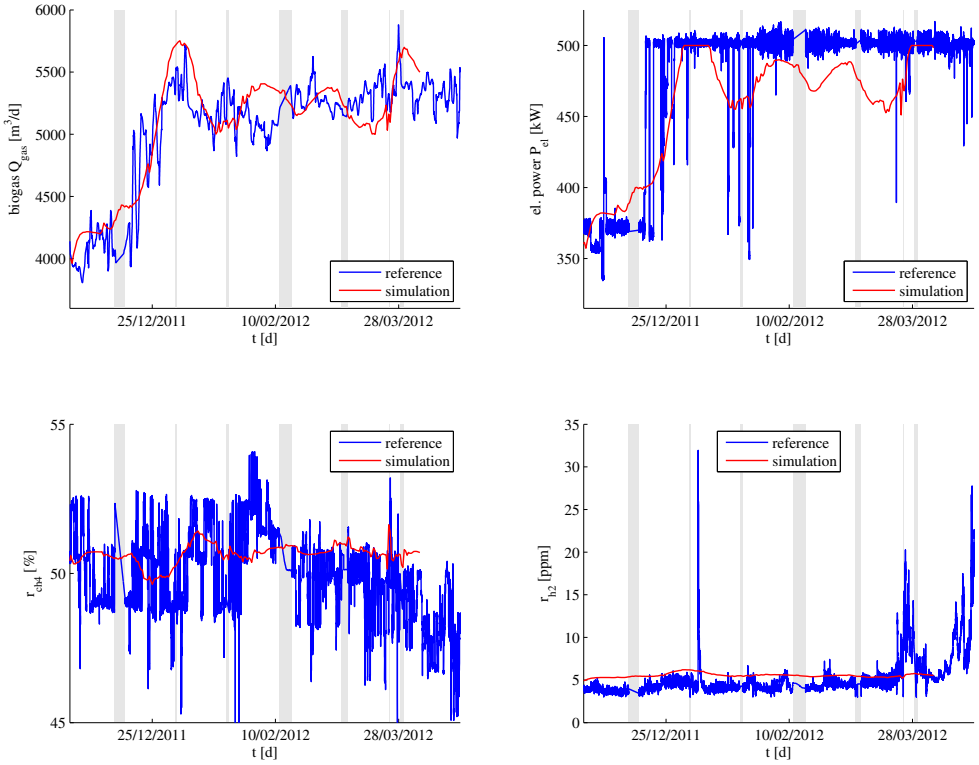

Figure 7.8: Calibration and validation results for the full-scale biogas plant: Online measurements. Top left: Biogas production Q_{gas}, top right: electrical power production P_{el}, bottom left: methane content r_{ch_4} in the produced biogas, bottom right: hydrogen content r_{h_2} in the produced biogas.

of the available online measurement data is often poor and probes not representative for the complete digester content. But there is no alternative to a complex gray box model. A simpler gray box model (created by omitting some equations) would be easier to calibrate, but would provide less information and a black box model would suffer even more from the insufficient data.

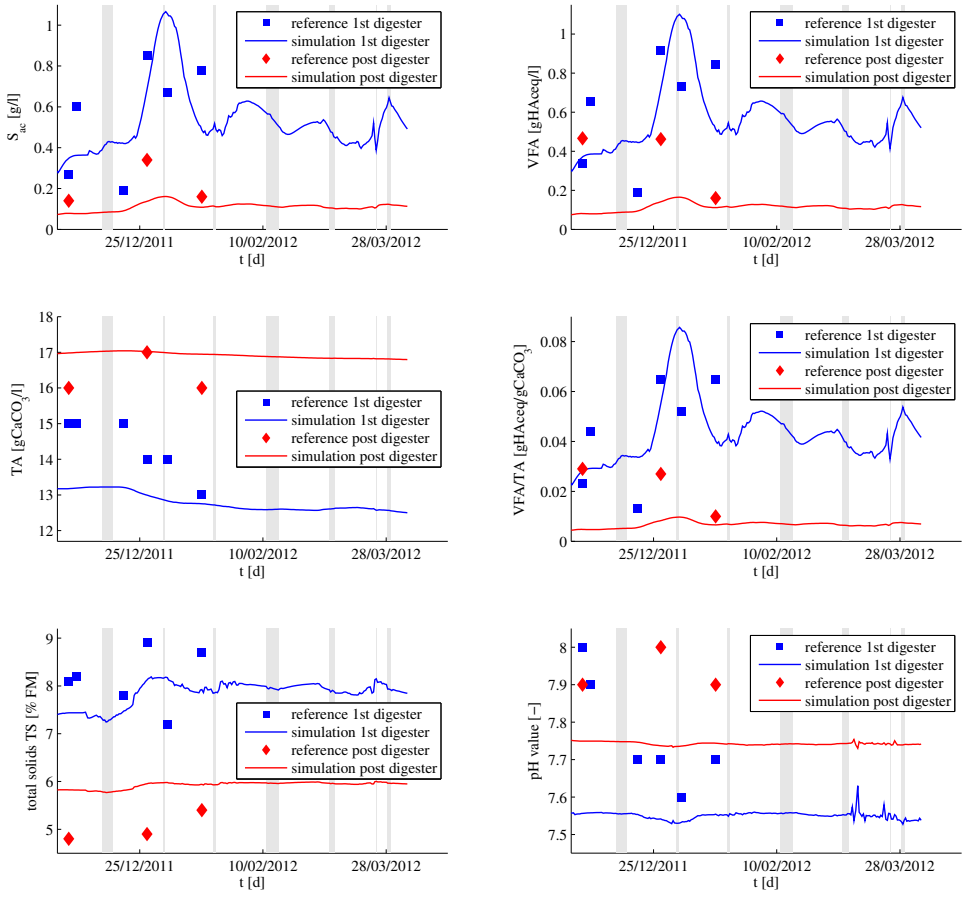

Figure 7.9: Calibration and validation results for the full-scale biogas plant: Offline measurements. Top left: acetic acid concentration S_{ac}, top right: volatile fatty acids VFA, middle left: total alkalinity TA, middle right: ratio of VFA to TA: VFA/TA, bottom left: total solids TS and bottom right: pH value

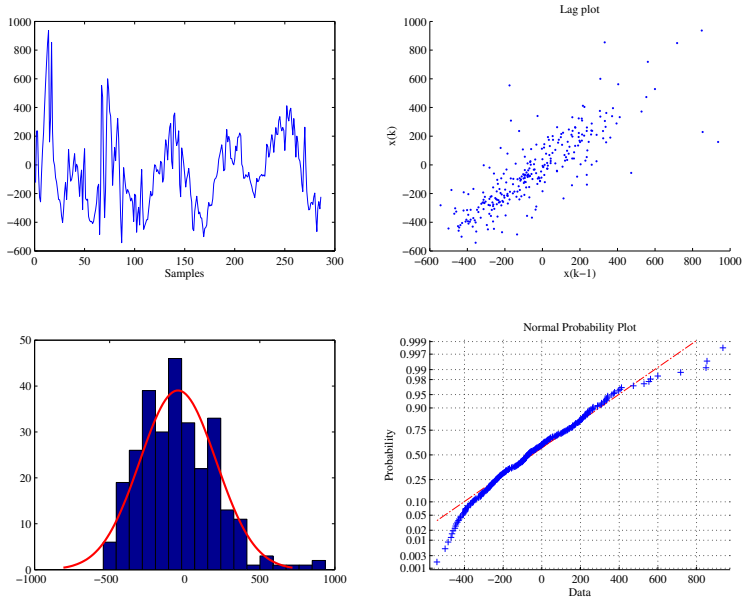

Figure 7.10: 4-plot analysis of model residuals for biogas flow rate Q_{gas}. In the lag plot $x(k)$ stands for the residual of the kth measurement.

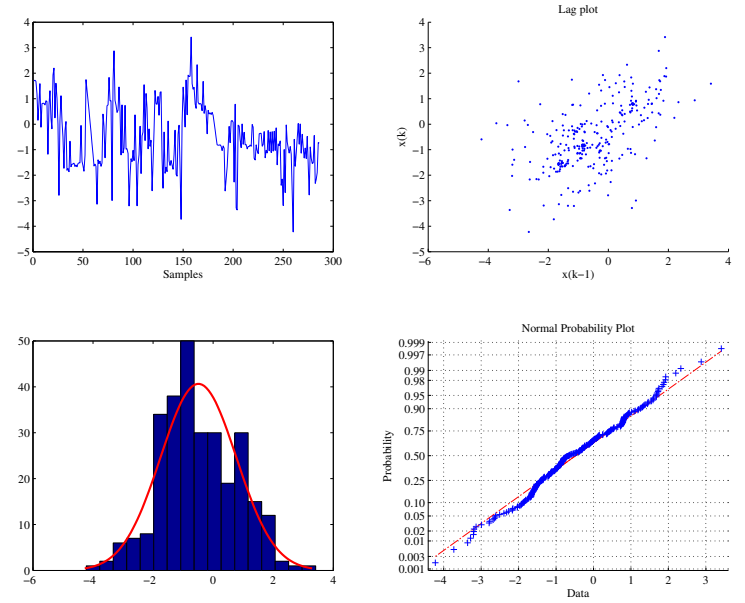

Figure 7.11: 4-plot analysis of model residuals for methane content r_{ch_4}. In the lag plot $x(k)$ stands for the residual of the kth measurement.

7.6 Summary and Discussion

In this chapter the simulation model of the biogas plant was proposed. Regarding the different models of the anaerobic digestion process here a pretty standard implementation of the ADM1 was used. The review in Section 7.1.1 revealed that there are much more sophisticated modeling approaches that use the ADM1 as well. As the focus of this thesis is on model predictive control and not on model development, this standard solution was used. Nevertheless, in the context of this thesis all other advanced model approaches could be used as well. This also includes models for different reactor types such as the UASB reactor. Especially the approach in Zaher et al. (2009) seems to be very well suited when the plant is fed with different substrates.

Also other parts of the model could be extended. For example a model for a gas storage tank or for the ensilage process could be added to make the model more real.

Compared with the complexity of full-scale biogas plants the ADM1 with all its extensions still is only a very crude approximation. Examples of influences on the biogas production process that are not modeled but certainly have an impact are:

- The concentration of all substances inside the digesters is far from equally distributed as is assumed by the ADM1.
- Environmental parameters such as pressure, temperature and gas transfer are assumed to be constant in the digester. Stacking a few ADM1 blocks vertically with sludge recirculation between these layers gradients of these parameters can be modeled, see (Ogurek and Alex, 2013). That way also floating layers can be simulated which could be modeled reducing the gas transfer rate. In (Ogurek and Alex, 2013) it was shown that these parameters have a significant influence on parameters such as VFA/TA, pH and CO_2 concentration.
- The presence or absence of trace elements that are needed by the biomass in the digesters is neglected.
- Adaptation of biomass to environmental changes such as seasonal influences are not handled here, but will be important in the future, when waste as dominating feed substance will be used.
- Non-ideal mixing of substrates. Here, the substrates are modeled as ideally mixed. In practice they are not, because liquid and solid substrates are often fed separately. In Zaher et al. (2009) all fed substrates are hydrolyzed independently which might be a more realistic modeling approach. In (Ogurek and Alex, 2013) the disintegration step is modeled separately for each substrate.

All this makes it very difficult to calibrate the model reliably at hand of the available measurements. Based on the noisy data it is often difficult to see whether there is a certain modeled cause changing the data or if the cause is not modeled. In the latter case it appears to the observer that the measured effects might be generated by stochastic

variations.
This model is used in Part III of this thesis. On the one hand it is used to create and validate the state estimator in Chapter 8 and on the other hand it is used to evaluate the developed RTO scheme in Chapter 9.